

In presenting the dissertation as a partial fulfillment of the requirements for an advanced degree from the Georgia Institute of Technology, I agree that the Library of the Institution shall make it available for inspection and circulation in accordance with its regulations governing materials of this type. I agree that permission to copy from, or to publish from, this dissertation may be granted by the professor under whose direction it was written, or, in his absence, by the Dean of the Graduate Division when such copying or publication is solely for scholarly purposes and does not involve potential financial gain. It is understood that any copying from, or publication of, this dissertation which involves potential financial gain will not be allowed without written permission.

Q . 1 . n
— . — Y —

LOW-FIELD DRIFT VELOCITY MEASUREMENTS
ON MASS-IDENTIFIED IONS IN NITROGEN

A THESIS

Presented to
The Faculty of the Graduate Division
by
George Emerson Keller

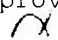
In Partial Fulfillment
of the Requirements for the Degree
Doctor of Philosophy in
the School of Physics

Georgia Institute of Technology

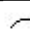
February, 1965

LOW-FIELD DRIFT VELOCITY MEASUREMENTS
ON MASS-IDENTIFIED IONS IN NITROGEN

Approved:



Chairman



Date approved by Chairman: Mar. 9, 1965

DEDICATION

This thesis is gratefully
dedicated to my wife Alice.

ACKNOWLEDGMENTS

The work described in this thesis was aided by a number of people. Chief among these was Dr. D. W. Martin, the author's thesis advisor, whose assistance was invaluable. Contributions were also made by Dr. E. W. McDaniel, Dr. W. S. Barnes, Dr. J. W. Hooper, and Dr. D. S. Harmer.

The author also wishes to thank Mr. L. J. Puckett, Mr. D. L. Albritton, Mr. W. C. Lineberger, Mr. J. R. Milford, and Mr. J. W. Martin for constructive discussions and other assistance. Special thanks are due Mr. J. B. Paine, who assisted the author's learning of techniques necessary to an effective research physicist.

This research was partially supported by the U. S. Air Force Office of Scientific Research under a grant administered by the Engineering Experiment Station of the Georgia Institute of Technology.

TABLE OF CONTENTS

	Page
DEDICATION	ii
ACKNOWLEDGMENTS	iii
LIST OF ILLUSTRATIONS	vi
SUMMARY	vii
Introduction	vii
The Present Experiment	ix
Conclusions	xi
Chapter	
I. INTRODUCTION	1
Basic Concepts	1
Summary of Mobility Theories	6
Summary of Mobility Measurements in Nitrogen	15
The Present Work	20
II. EXPERIMENTAL APPARATUS AND METHOD	23
Drift Field and Ion Source	26
Gas Handling System	32
Mass Spectrometer and Counting Equipment	37
Experimental Techniques	38
III. RESULTS	41
Factors Affecting the Accuracy of the Measurements	41
The Measurements	48
IV. CONCLUSIONS	64
V. RECOMMENDATIONS	66
Appendices	
A. ERRORS IN PRESSURE MEASUREMENTS INTRODUCED BY COLD TRAPPING A MERCURY MANOMETER	68
B. MATHEMATICAL FORM AND EVALUATION OF THE DATA	72

TABLE OF CONTENTS (Continued)

	Page
C. ASPECTS OF RARIFIED GAS DYNAMICS RELEVANT TO THE PRESENT INVESTIGATION	84
BIBLIOGRAPHY	88
VITA	93

LIST OF ILLUSTRATIONS

Figure	Page
1. Previous Measurements of the Drift Velocity of Nitrogen Ions in Nitrogen at 0°C	17
2. Overall View of the Experimental Apparatus.	24
3. Schematic View of Internal Components of the Apparatus. . .	25
4. View of Source, Source Supporting Structure, and Drift Field Electrodes	27
5. View of Source	29
6. Source Circuitry	30
7. Drift Velocity Data for Mass-Identified Ions in Nitrogen. .	49
8. Arrival-Time Spectra - Low Pressure	50
9. Arrival-Time Spectra - High Pressure	51
10. Comparison of Mass-Analyzed Drift Velocity Data N_1^+ and N_2^+	53
11. Comparison of Mass-Analyzed Drift Velocity Data N_3^+ and N_4^+	54
12. Comparison of Present Data with Data of Other Workers . . .	55
13. Tube-in-Tube Cold Trap	71
14. Contour of Integration	80

SUMMARY

Introduction

If ions of a given kind move in a gas under the influence of a static, uniform electric field, and if the energy they acquire from this field is small with respect to their thermal energy, then their drift velocity in the direction of the field is proportional to the field strength. This fact may be expressed by the equation

$$v_d = K E$$

where v_d is the drift velocity, E is the field strength, and K is a constant called the mobility of the ions. This relationship is predicted by theory and has been verified experimentally.

A knowledge of the mobilities of ions in gases is important for several reasons. First, mobilities shed light on the ion-molecule forces at greater separation distances than are accessible in scattering experiments. Second, knowledge of the mobility of an ion in an experiment in gaseous electronics helps to identify the ion. Third, mobilities enter into the calculation of diffusion coefficients, dispersion due to mutual repulsion, ionic recombination, and the characteristics of electrical discharges.

Classical mobility theories based on the kinetic theory of gases were developed decades ago by Langevin, Chapman, Enskog, and others. Their theories are applicable where E/p (p is the pressure of the gas)

is small enough that the energy acquired from the drift field is small with respect to the thermal energy of the ion. They showed that the drift velocity should be proportional to E/p and proportional to $\sqrt{\frac{m+M}{mM}}$, where M is the mass of a gas molecule and m is the mass of the ion. Wannier later extended the theory to the high E/p region where the energy acquired from the field is no longer negligible. He was able to show that in this region the drift velocity should in general be proportional to $\sqrt{E/p}$.

The general quantum mechanical theory of mobilities has been discussed more recently by Dalgarno, McDowell, and Williams. Quantum theory predicts essentially the same results as classical theory except when specific quantum effects are operative. These effects come into play when the gas temperature is very low and when the cores of the ion and the gas molecule are identical. In the latter instance, resonance charge transfer and other symmetry effects are quite important and must be considered. Indeed, the present experiment demonstrates the strong retarding effect of resonance charge transfer on the mobility of N_2^+ ions moving through the parent gas.

The proportionality of the low-field drift velocity to E/p was experimentally verified by Mitchell and Ridler thirty years ago for various ions in nitrogen. In these experiments Mitchell and Ridler found anomalously low drift velocities for nitrogen ions in nitrogen. They considered resonance charge exchange to be the most probable explanation.

J. A. Hornbeck was the first to demonstrate experimentally that at high E/p the drift velocity of ions was proportional to $\sqrt{E/p}$. In this work, he studied noble gas ions in their parent gases.

In the last dozen years Varney and his co-workers have extensively studied the problem of drift velocity of the ions of nitrogen. In 1953 Varney observed that as E/p declined, the drift velocity of ions in nitrogen declined smoothly to about E/p_0 of 90 volts per cm-torr, at which point v_d started rising toward a local maximum at about 60 volts per cm-torr. Here p_0 is the "reduced pressure" defined by the equation

$$p_0 = p \frac{273}{T}$$

in which T is the absolute temperature of the gas and p is the pressure at which the measurement is made. Varney thought that in his pressure range and for E/p_0 above 90 volts per cm-torr, the most abundant ion was N_2^+ , and that below an E/p_0 of 60 volts per cm-torr it was N_4^+ , with some mixture of these ions present at intermediate values of E/p_0 . Thermodynamic arguments seemed to support this idea. By 1963 his apparatus had been refined enough for him to obtain two separate drift velocity curves, which he labeled as curves for N_2^+ and N_3^+ . However, other workers with mass spectrometers had seen four ions in nitrogen: N_1^+ , N_2^+ , N_3^+ , and N_4^+ . Clearly drift velocity measurements on simultaneously mass-identified ions were required if the situation were ever to be understood.

The Present Experiment

For the present experiment an apparatus has been developed with which it is possible to measure the drift velocity of an ion while simultaneously identifying its mass. This arrangement permits measurements to be made for one type of ion in the presence of several others.

The apparatus consists of a three-foot-long gas-filled drift tube linked to a mass spectrometer through differentially pumped chamber. This "drift tube mass spectrometer" differs in its source and source support from the apparatus used in earlier work in this laboratory. The present apparatus has an electron-bombardment ion source which is movable along the axis of the tube so that runs can be made that are essentially identical except for source position. Bursts of ions from the source drift down the tube under the influence of a weak axial electric field and are swept out through an exit aperture into the differentially pumped chambers. After passing through these chambers, the ions are accelerated into a mass spectrometer and detected by an ion multiplier. The pulses from this multiplier are sorted by a twenty-channel time analyzer from whose output can be calculated the drift velocities of the ions. Implied mobilities for the ions in nitrogen can be calculated from these drift velocities. Drift fields of one to six volts/cm and pressures from 50 μ to 200 μ (0.05 to 0.20 torr) have been used in this experiment.

The maximum available drift distance in this apparatus is 34 cm, much longer than is customary for other mobility measurements. This longer distance permits accurate measurements of the drift distance and the drift field used. The longer drift distance also means that the total drift times to be measured are much greater than those of most other experimenters, the drift times here ranging from 70 to 3500 μ sec. Such times are easily measured with conventional circuitry. For additional accuracy, only differences in mean drift times from two source positions are used, so that end effects do not affect the measurements.

The absolute error in the time measurements in the present experiment is not believed to exceed two per cent.

A McLeod gauge is used to measure the pressure of the gas during a run. This gauge is cold-trapped to keep mercury vapor out of the drift tube. The trap is designed to eliminate effects of thermal transpiration, and the pressure to be measured is high enough that the Gaede mercury-pumping effect causes errors of less than two per cent. However, it is still believed that the major error in the experiment lies in the pressure measurement. The relative values of the drift velocity data for the various ions are not affected, but their absolute values may be in error as much as five or six per cent.

Conclusions

a. In the experiment described here, four nitrogen ions are present: N_1^+ , N_2^+ , N_3^+ , and N_4^+ .

b. For all available conditions N_1^+ is the most abundant ion. This fact is probably the result of the use of electrons of 75-eV energy in the electron bombardment ion source. Most experiments utilize a smaller electron energy, in some cases less than the 24.3 eV necessary for direct production of N_1^+ ions.

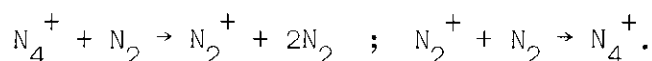
c. The shapes of the arrival time spectra obtained suggest that the N_1^+ ions that are seen are formed only at the source and not farther down the drift tube by secondary processes involving other ions.

d. Over wide limits of pressure and for E/p_0 between 7 and 70 volts/cm-torr the log-log plot of v_d vs E/p_0 for N_1^+ is straight and has a slope of unity. The shape and position of this plot imply a zero-field,

reduced mobility for N_1^+ of $2.47 \text{ cm}^2/\text{V-sec}$. (The "reduced mobility" is the mobility referred to the standard conditions of 760 torr gas pressure and 0°C gas temperature.)

e. Of the other ions (N_2^+ , N_3^+ , and N_4^+), N_2^+ is the most abundant for high E/p_0 , especially for pressures less than about 100μ . N_3^+ and N_4^+ , in about equal numbers, take over from N_2^+ for low E/p_0 provided that the pressure is greater than about 145μ .

f. The shapes of the arrival time spectra show that N_2^+ and N_4^+ are closely interrelated. The widths and overlap of these peaks suggest a reaction scheme of the type proposed by Varney in 1953:



g. The shapes of the arrival time spectra suggest that there may be some reactions between N_3^+ and N_2^+ , and between N_3^+ and N_4^+ .

h. Provided that the gas pressure is less than about 100μ , the log-log plot of v_d vs E/p_0 for N_2^+ is straight and has a slope of unity for E/p_0 less than 30 volts/cm-torr. This plot is consistent with a zero-field, reduced mobility for N_2^+ of $1.44 \text{ cm}^2/\text{V-sec}$. For pressures greater than about 145μ , the plot of v_d vs E/p_0 for N_2^+ rises with greatly increased scatter toward the plot of v_d for N_4^+ for E/p_0 less than 30 volts/cm-torr.

i. Provided that the gas pressure is greater than about 145μ , the log-log plot of v_d vs E/p_0 for N_4^+ is straight and has a slope of unity for E/p_0 less than 30 volts/cm-torr. This plot is consistent with a zero-field, reduced mobility for N_4^+ of $1.84 \text{ cm}^2/\text{V-sec}$. For pressures

less than about 100μ , the plot of v_d vs E/p_o for N_4^+ falls with increased scatter toward the plot of v_d for N_2^+ for E/p_o less than 30 volts/cm-torr.

j. In no available pressure regime is the slope of the log-log plot of v_d vs E/p_o for N_3^+ equal to unity, so that no unique reduced mobility is implied, though for the highest pressures used (150μ - 200μ) the drift velocity plot is straight. For pressures less than 100μ , the plot of v_d for N_3^+ falls toward the plot for N_4^+ .

CHAPTER I

INTRODUCTION

Basic Concepts

Mobility

Many years ago investigators became aware of the fact that under certain circumstances a gas can act as a conductor. In fact, it was in 1785 that Coulomb presented conclusive evidence that at least part of the charge lost by an insulated, charged body over a long period of time is conducted away by the surrounding air. Since then there have been many investigations of the electrical conductivity of gases.

One phase of this investigation has been the study of the migration of ions through a gas under the influence of an externally applied electric field. The average velocity of ions in the direction of the applied electric field is called their drift velocity, and many different experiments have been conducted to measure drift velocities of various ions in a variety of gases.^{1,2,3}

It was soon found that when the energy acquired from the field was small compared to the ion's thermal energy, the drift velocity v_d of an ion in a gas at constant pressure was proportional to the drift field intensity. This fact can be expressed by the equation

$$v_d = K E , \quad (1)$$

where E is the drift field intensity and K is a constant called the

mobility. K is usually expressed in units of square centimeters per volt per second. For ease of comparison, a mobility value quoted in the literature is usually a reduced mobility K_o , defined by the equation

$$K_o = K \frac{p}{760} \frac{273}{T} , \quad (2)$$

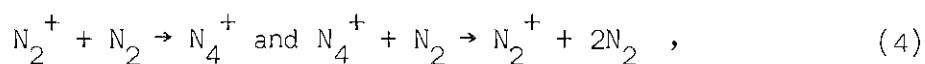
in which p is the gas pressure at which the measurement is performed and T is the temperature of the gas in degrees Kelvin.

The quantity that determines the validity of the mobility concept for a given ion-gas combination at a given gas temperature is E/p . For small values of E/p , the energy acquired by the ions from the electric field is small compared with their thermal energy, with the result that the velocity distribution of the ions is nearly the Maxwell distribution, and the drift velocity is directly proportional to the electric field intensity. For large values of E/p , however, the ions acquire a significant amount of "field energy," so that the ionic velocity distribution is not close to Maxwellian, v_d is no longer proportional to E/p , and the concept of a mobility breaks down. In the literature, the drift velocity or the mobility of an ion is usually plotted versus E/p_o , where p_o is the reduced pressure defined by the equation

$$p_o = p \frac{273}{T} . \quad (3)$$

The mobility of an ionic species is a characteristic of the drift of that kind of ion through a particular gas. If ions of a given type drift through a gas, some of the ions are likely to be lost through reactions forming ions of a different type. Even if this occurs, the

mobility of the remaining original-type ions is still a meaningful quantity and can be measured. However, if the secondary ions which were formed react with the gas to produce new ions of the original type, then it may be impracticable to measure the mobility for either of the ion types, since some of their number are disappearing and reappearing continually. For example, in 1953 Varney⁴ proposed a pair of reactions in nitrogen,



which could mask the true drift behavior of both N_2^+ and N_4^+ . The results of the present work seem to support this type of interpretation of the behavior in nitrogen.

Diffusion Coefficient

The phenomenon of diffusion had been studied quantitatively long before quantitative studies were first made on the drift of ions through gases. The kind of diffusion most relevant to the present discussion is mutual diffusion, which is the net transport of particles of one kind through a medium composed of particles of a different kind because of a gradient in the concentration of the particles of the first kind. The effect of mutual diffusion is to tend to distribute the diffusing particles evenly throughout the medium through which the diffusion occurs.

The rate of diffusion of ions in a gas is proportional to the magnitude of the concentration gradient, and the diffusive flow occurs in the opposite direction to the gradient. The constant of proportionality is called the diffusion coefficient, D , and is usually expressed in units of square centimeters per second. The proportionality is expressed in Fick's law of diffusion

$$\vec{J} = - D \vec{\nabla} n , \quad (5)$$

where \vec{J} is the ionic current density, and $\vec{\nabla} n$ is the gradient of the ionic number density.

The mobility is generally easier to measure than the diffusion coefficient, and the most accurate diffusion coefficients have been obtained from mobility measurements. This indirect determination of D is possible because at low E/p , K and D are related by the equation

$$\frac{K}{D} = \frac{e}{k T} . \quad (6)$$

This relationship is exact for certain ion-molecule interaction potentials and at worst is in error by only a few per cent. In this equation e is the electronic charge, and k is Boltzmann's constant. A derivation of this equation is available elsewhere.^{5,6}

Coefficient of Ambipolar Diffusion

Up to this point, it has been assumed that the ion (or electron) density in the gas was low enough to permit the neglect of interactions among the charges. There are occasions when this is not the case, however, and the ionic diffusion must be analyzed rather differently. In a highly ionized gas, the number densities of positive ions and of electrons must be approximately equal. Any tendency for this situation to change leads to a space charge field which restores the balance. Thus the net flow of ions and of electrons is the same. This kind of diffusion is termed ambipolar because it is the same for charged particles of both signs.

If the gas pressure is high enough to cause the particles to make frequent collisions, the velocity of ambipolar diffusion, v_a , is given by the equations

$$v_a = - \frac{D^+}{N} \frac{dN}{dx} + K^+ E \quad (7a)$$

and

$$v_a = - \frac{D^-}{N} \frac{dN}{dx} - K^- E , \quad (7b)$$

where the superscripts + and - refer to the positive ions and the electrons respectively, N is the common number density of positive ions and electrons, and E is the intensity of the electric field set up by the attempted separation of the charges. If E is eliminated, v_a can be expressed by the equation

$$v_a = - \frac{D^+ K^- + D^- K^+}{K^+ + K^-} \frac{1}{N} \frac{dN}{dx} , \quad (8)$$

and the diffusion of the system is seen to be characterized by the coefficient of ambipolar diffusion, D_a , defined by the equation

$$D_a = \frac{D^+ K^- + D^- K^+}{K^+ + K^-} . \quad (9)$$

The temperature of the positive ions, T^+ , and the temperature of the electrons, T^- , are not necessarily the same. If it is assumed that $T^- \approx T^+ \approx T$ and $K^- \gg K^+$, the proportionality of K to D can be used to show that

$$D_a \approx \frac{2kT}{e} K^+. \quad (10)$$

Thus measurements of the coefficient of ambipolar diffusion in a gas can yield a mobility for the ions in that gas. Measurements of the ambipolar diffusion coefficient are generally carried out in the decaying afterglow of a microwave discharge, and experimental conditions can usually be imposed to insure that the electron and ion temperatures are approximately equal so that the relationship between D_a and K^+ displayed above is valid. Unfortunately, it is seldom the case that there are few enough stable species of positive ions in a gas that unambiguous ion identification is possible.

Summary of Mobility Theories

Classical Theories

Langevin. In 1903 Langevin⁷ published his simple mean-free-path mobility theory, which was based on the recently developed kinetic theory of gases. He assumed that there was a distribution of free paths, that the ions and molecules were rigid elastic spheres, that E/p was low, and that the ionic density was low enough that ion-ion interactions could be neglected. His result for the mobility can be expressed by the equation

$$K = \frac{e \lambda}{m \bar{v}}, \quad (11)$$

where e is the charge of the electron, λ is the mean free path, m is the common molecular and ionic mass, and \bar{v} is the mean thermal velocity.

A similar calculation⁸ which assumes a distribution of velocities and the ionic mass m not necessarily equal to the molecular mass M yields

$$K = 0.815 \frac{e L}{M v_R} \left(1 + \frac{M}{m}\right)^{\frac{1}{2}}, \quad (12)$$

where v_R is the rms thermal velocity of the molecules and

$$L = \frac{1}{\pi N D_{12}^2}. \quad (13)$$

Here N is the molecular number density and D_{12} is the sum of the ionic and molecular radii. This expression for the mobility is deficient in several respects⁹; among other faults, the mobility predicted is about four times too large. It was apparent that a mechanism needed to be added to the theory to shorten the ionic mean free path. The polarization attraction between ions and molecules is such a mechanism and was investigated by Langevin in 1903.⁷

In 1905 Langevin¹⁰ published a much improved mobility theory. He assumed a Maxwellian distribution of velocities, low E/p , low ionic density so ion-ion interactions could be neglected, and inverse-fifth-power polarization attraction in addition to rigid sphere repulsion. Using the momentum transfer method, he showed that

$$K = \frac{3}{16 Y \sqrt{(k-1)p}} \left(1 + \frac{M}{m}\right)^{\frac{1}{2}}, \quad (14)$$

where M is the molecular mass, p is the gas density, m is the ionic mass and k is the dielectric constant of the gas. (The presence of the

dielectric constant in this expression is significant, for the dielectric constant is a measure of the polarizability of the gas and therefore is a measure of the relative importance of the polarization attraction.) The quantity Y is a function of a parameter μ which is defined by the equation

$$\mu = \left[\frac{(k-1) e^2}{8\pi p D_{12}^4} \right]^{\frac{1}{2}}, \quad (15)$$

where p is the pressure of the gas. In the limit of negligible polarization effects, Eq. (13) assumes the form

$$K_e = \frac{0.75 e}{D_{12}^2 \sqrt{8\pi p \rho}} \left(1 + \frac{M}{m} \right)^{\frac{1}{2}}. \quad (16)$$

When the polarization attraction dominates, Eq. (13) becomes

$$K_p = \frac{0.505}{\sqrt{(k-1) \rho}} \left(1 + \frac{M}{m} \right)^{\frac{1}{2}}. \quad (17)$$

In 1926 Hassé¹¹ called attention to Langevin's 1905 paper, which had been almost unnoticed since its publication. Hassé reevaluated the numerical part of Langevin's calculations, and for the polarization limit obtained the equation

$$K_p = \frac{0.5105}{\sqrt{(k-1) \rho}} \left(1 + \frac{M}{m} \right)^{\frac{1}{2}}. \quad (18)$$

Chapman-Enskog. There are two main parts to the rigorous calculation of the drift motion of ions through a gas in an applied electric field. The first part consists of the evaluation of the differential cross section for elastic scattering of an ion by a gas molecule. In principle, the second part of the problem consists of determining the velocity distribution function for the ions and then taking the first moment of this function, which is the desired drift velocity of the ions in the direction of the electric field. In practice, the drift velocity for ions is always obtained by assuming a velocity distribution and calculating the drift velocity directly through the use of the differential cross section in a lengthy averaging computation. The second part of the overall calculation is recognized as a problem in the kinetic theory of gases.

A few years after Langevin's work, Chapman¹² and Enskog¹³ independently developed a rigorous kinetic theory for dilute (spherically symmetric) monatomic gases. One of their main objectives was to establish a formalism for accurate computation of transport coefficients for neutral molecules. Although Chapman and Enskog did not treat ions explicitly, their results can be applied to the calculation of the low-field mobility of ions.

Chapman and Enskog assumed that all collisions were binary, that the gradients of all physical quantities were small, and that the gas pressure and temperature were constant in space and time. They obtained an expression for the mutual diffusion coefficient, D_m , for two different types of molecules. Replacement of the molecule-molecule interaction potential in this expression by a suitable ion-molecule interaction

potential enables one to calculate the diffusion coefficient for ions in a gas; the ionic mobility can be obtained from the ionic diffusion coefficient by use of Equation (6).

Chapman and Enskog's expression for the mutual diffusion coefficient has the form

$$D_m = \frac{3\sqrt{\pi}}{16} \left(\frac{2kT}{M_r} \right)^{7/2} \frac{1 + \epsilon_0}{(N_1 + N_2) P_{12}}, \quad (19a)$$

where P_{12} is a collision integral given by the expression

$$P_{12} = \int_0^\infty v_o^5 q_d(v_o) \exp\left(-\frac{M_r v_o^2}{2kT}\right) dv_o \quad (19b)$$

and $q_d(v_o)$ is the diffusion cross section, defined by the equation

$$q_d(v_o) = 2\pi \int_0^\pi [1 - \cos \Theta] I_s(\Theta) \sin \Theta d\Theta. \quad (19c)$$

For strictly classical calculations, this equation may take the form

$$q_d(v_o) = 2\pi \int_0^\infty [1 - \cos \Theta(b)] b db. \quad (19d)$$

In these equations M_r is the reduced mass of the ion-atom system, N_1 is the number density of the ions, N_2 is the number density of the gas, v_o is the relative velocity of approach at a large separation distance, ϵ_0 is a second-order correction which is usually small¹², Θ is the scattering angle in the center of mass frame, $I_s(\Theta)$ is the elastic scattering cross section per unit solid angle, and b is the (classical) impact parameter. The relationship of Θ to b or $I_s(\Theta)$ is a function of

the detailed model of the collision mechanism used, that is, of the force law of the ion-atom interaction.

Strictly speaking, quantum mechanics should be used to calculate $I_s(\Theta)$, but usually classical mechanics provides an excellent approximation except for very small values of Θ . Equations (19) show that $I_s(\Theta)$ appears only in the diffusion cross section, q_d , and that in q_d , the multiplicative factor $(1 - \cos \Theta)$ discriminates heavily against small-angle scattering contributions. The presence of the $(1 - \cos \Theta)$ weighting factor causes the classical calculation of q_d to be valid in most instances and explains the success of the prequantum mechanics transport theories. The necessity for applying quantum mechanics in special instances will be discussed later.

Kihara¹⁴ showed how the methods of Chapman and Enskog could be extended to include the effects of nonvanishing electric fields as well as higher order approximations to the coefficients involved.

In 1958 Mason and Schamp¹⁵ used Kihara's extension of the Chapman-Enskog theory to obtain the second and third order approximations to the mobility of gaseous ions in a weak electric field as a function of temperature and field strength. They assumed that there was no charge exchange between the ions and gas atoms, that there was no clustering of neutral molecules to ions, and that quantum effects could be neglected. They expressed the mobility in a series in ascending powers of the square of the field strength. The collision integrals which entered into the coefficients of the series were evaluated by numerical integration for a force law which took into account the charge-induced dipole, charge-induced quadrupole, the London dispersion forces, and an

inverse twelfth power repulsion potential. The agreement between this theory and the experimental results compared with it was good except for those cases in which clustering was to be expected.

Wannier. Another modern theoretical treatment of the mobility problem is that of Wannier¹⁶, whose work is of particular importance because it relates mainly to the high-field region, which had not been adequately treated by previous investigators. Wannier assumed that the ion density was low and that the ion-atom collisions were elastic.

In one part of his discussion, Wannier used dimensional analysis to investigate two limiting conditions of the ionic drift: The case of a constant mean free path (which applies to pure hard sphere scattering), and the case of a constant mean free time (which applies when polarization forces dominate). For low E/p_0 he was able to show that

$$v_d \sim \frac{E}{p} \quad (20)$$

for both constant mean free path and constant mean free time. For high E/p_0 he was able to show that

$$v_d \sim \frac{E}{p} \quad (21)$$

for constant mean free time and

$$v_d \sim \left(\frac{E}{p}\right)^{\frac{1}{2}} \quad (22)$$

for constant mean free path. Equation (22) expresses the same relationship that Sena¹⁷ had found. Sena had assumed that charge exchange of the ions is the predominating process in the interaction between ions and molecules. Comparison with the measurements of Hornbeck^{18,19} and Varney²⁰

showed that the high field dependence was correctly predicted by Eq. (22) for noble gas ions in their parent gases. The proportionality of v_d to E for low E/p_0 means that a log-log plot of v_d vs E/p_0 should be straight and should have a slope of unity at low E/p_0 . Such a plot permits a mobility to be extracted from drift velocity data easily by use of Eqs. (1) and (2) since the mobility is constant in the low E/p_0 region.

Quantum Mechanical Theory

The general quantum mechanical mobility theory has been discussed and extended by Dalgarno, McDowell, and Williams^{21,22} both for ions in unlike gases and for ions in their parent gases, wherein symmetry effects can arise.

The result of Chapman and Enskog, Eq. (19), is satisfactory for the case of low gas temperature or the case of identical cores of the ion and gas atom only if quantal methods are used to evaluate $q_d(v_0)$, Eq. (19c). The diffusion cross section $q_d(v_0)$ can be expressed by quantal methods in terms of a series of phase shifts, which depend on a detailed knowledge of the interaction potentials. As expected, these quantum mechanical calculations predict essentially the same results as classical theory except when specific quantum effects are operative.

A quantum mechanical mobility calculation by Dalgarno²² for the case of N_2^+ in nitrogen yields a zero-field, reduced mobility of 1.5. This calculation is important, for it is the only calculation that has come to light which considers resonance charge exchange for the case of N_2^+ in nitrogen.

Most discussions of the mobility of ions in molecular gases have been based on the assumption that it is permissible to average the

interaction over all orientations before computing the appropriate elastic collision cross section. Arthurs and Dalgarno²³ have developed a theory of scattering in which this assumption was not made, and they have derived a formula for the low-field mobility of an ion in a diatomic gas. Quantitative calculations of mobilities in H_2 and D_2 at low temperatures are presented. These calculations show that unlike atomic gases, in which the mobility tends to become independent of the gas temperature as the temperature decreases, molecular gases should have a mobility which decreases as the temperature decreases. For these calculations, only the lead term of the interaction potential was retained, so the results are valid only in the limit of vanishing temperature. It is stated that inclusion of polarization terms in the potential will enable calculations to be made for a gas at room temperature.

Recently Dalgarno and Henry²⁴ have analyzed the customary interpretation of experimental data on transport properties and scattering in molecular gases. The customary interpretation assumes a spherically symmetric interaction potential and single channel (elastic) scattering. This procedure is shown to be justifiable as a first approximation provided it is recognized that the generalization of transport theory to molecular gases involves the replacement of elastic cross sections by total cross sections, and that, in fact, beam scattering data refer to total cross sections and not elastic cross sections. Dalgarno and Henry show that consideration of the distinction between total and elastic cross sections implies that there might be a marked difference between low-temperature mobilities in atomic and in molecular gases, as had been predicted by Arthurs and Dalgarno from scattering considerations alone.

Summary of Mobility Measurements in Nitrogen

One of the first mobility measurements made in nitrogen was that of Tyndall and Powell in 1930²⁵. They used the "four-gauze," or "four-grid," electrical shutter method of measurement that has recently been used by Beaty²⁶ for very precise measurements in argon. They obtained a value for the zero-field, reduced mobility of ions in nitrogen of 1.95 if it is assumed that their experiment was conducted at a temperature of 22°C.

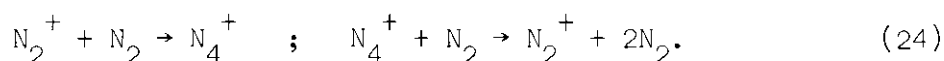
In 1932 Bradbury²⁷ used the four-gauze method to measure the mobility of ions in very pure nitrogen. He was quite thorough in his gas handling and purification, and obtained a limiting, zero-field mobility value of 2.09 in the purest gas he could prepare. This value reduced to standard temperature from the 22°C used in the experiment becomes 1.93.

In 1934 Mitchell and Ridler²⁸ used the four-gauze method to measure the mobilities of a large number of different ions in nitrogen. They found that in nitrogen gas the mobility of an ion of atomic weight m is given by the equation

$$K = B \left(1 + \frac{28}{m}\right)^{\frac{1}{2}}, \quad (23)$$

where B is a numerical constant. The only ions whose mobility differed significantly from this prediction were those of nitrogen itself, which were slower than would have been expected from this equation. The results of Mitchell and Ridler for nitrogen ions in nitrogen will be presented in Chapter III. The zero-field mobility for nitrogen ions, reduced to standard pressure and 293°K, was found to be 2.67. This mobility, reduced to 760 torr and 273°K is 2.49.

In 1953 Varney⁴, using the apparatus developed by Hornbeck²⁹, found evidence that more than one kind of ion was contributing to the measured drift velocities of nitrogen ions in the parent gas. His results are shown in Figure 1. He proposed that at low E/p_0 the ions were largely N_4^+ , at high E/p_0 they were N_2^+ , and in the intermediate region each ion changed many times from N_2^+ to N_4^+ and back. This reaction scheme can be expressed by the equations



At low E/p_0 , the first reaction predominates; at high E/p_0 , the second reaction predominates.

In 1957 Kovar, Beaty, and Varney³⁰, using the apparatus of Beaty³¹, measured the drift velocities of ions in nitrogen at various temperatures. Their plot of the drift velocity versus E/p_0 showed that an increase in temperature lowered the drift velocities. Each of their curves exhibited the ionic transition that had been found by Varney.

In 1959 Varney³² presented a physico-chemical analysis of the available drift velocity data for nitrogen which supported the N_2^+ , N_4^+ reaction scheme he had proposed. This analysis also yielded a value of 0.50 eV for the binding energy of N_4^+ ions against dissociation into N_2^+ and N_2 .

By 1963 Varney and Dahlquist^{33,34,35} had developed a new apparatus with a glow-discharge source, electronic ion shutters, and much improved timing. They were able to separate drift velocity data for ions whose identity they thought be be N_2^+ and N_3^+ . The zero-field, reduced mobility for N_2^+ was about 1.75 and for N_3^+ was about 2.9.

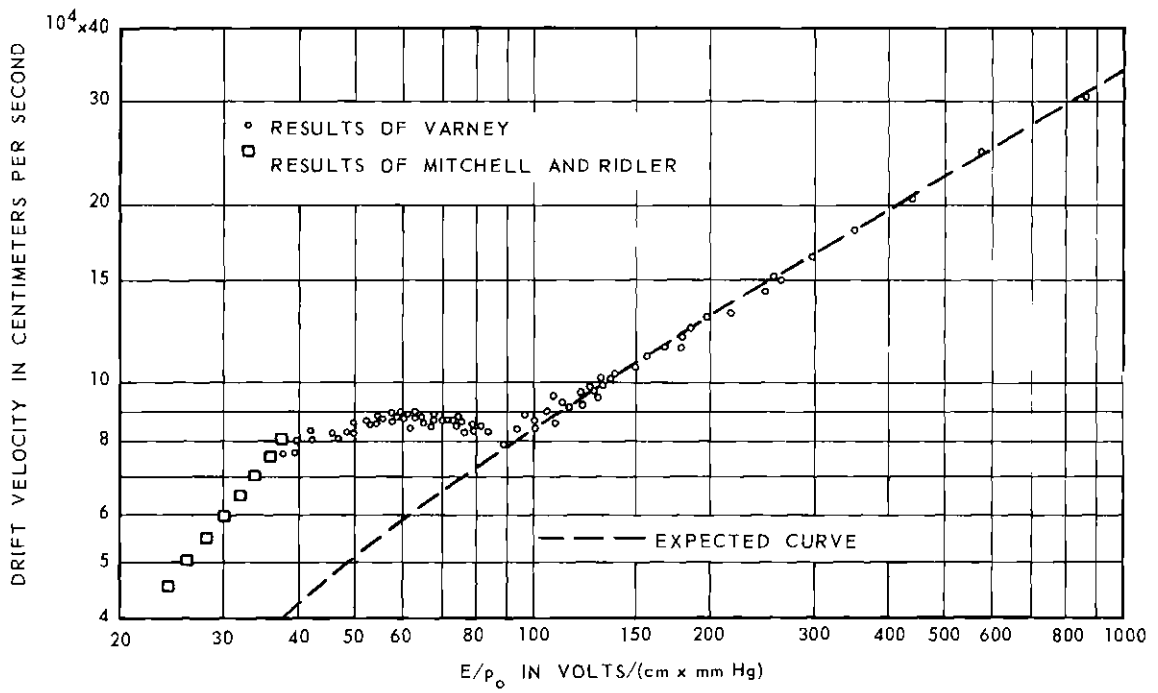


Figure 1. Previous Measurements of the Drift Velocity of Nitrogen Ions in Nitrogen at 0°C.

In 1964 Woo³⁶ reported some mobility measurements with an apparatus very similar to Dahlquist's. He used a thermionic ion source, improved electronics, more precisely defined and measured final drift space, and an advanced technique of analysis of the data. His apparatus had a 9.3 mm drift space; his data were taken for p_0 usually between 0.471 torr and 1.5 torr, and for E/p_0 as low as 8 and as high as 200 V/cm-torr. The mass identification of his ions was based on the mass spectrometric work of others. He saw no ions which he thought to be N_4^+ for any E/p_0 and no ions believed to be N_2^+ below an E/p_0 of about 50, for at that value of E/p_0 N_2^+ was apparently being converted to N_3^+ . He was able to obtain drift velocity data at low E/p_0 for only two ions, which he supposed to be N_1^+ and N_3^+ ; the zero-field, reduced mobilities inferred from these data were 3.4 for N_1^+ and 2.9 for N_3^+ .

Several other investigators have been able to infer mobilities for the ions in nitrogen from their work. In 1957 Vogel³⁷ measured the zero-field, reduced mobility of ions in nitrogen to be 2.5 cm²/V-sec. In 1963 Davies et al.³⁸ reported that their mobility measurements yielded a zero-field, reduced mobility for ions in nitrogen of 2.5. Zipf³⁹ has been able to imply from his investigations on the decaying afterglow of a microwave discharge that the zero-field, reduced mobility for ions in nitrogen is 2.4.

The first published reports on mobility experiments in which the ions were mass-analyzed while their drift velocities were measured were made at the Sixth International Conference on Ionization Phenomena in Gases (Paris, 1963). Preliminary results of the present experiment⁴⁰ and the results of McAfee and Edelson⁴¹ as well were reported at this meeting.

McAfee and Edelson used a Townsend-discharge mobility tube¹ which had been joined to a time-of-flight mass spectrometer. The development of their apparatus was concurrent with the development of the apparatus of the present experiment. In their apparatus, a light pulse from the spark source causes photoelectrons to be emitted from the cathode of the Townsend cell. These electrons are accelerated through the gas-filled cell by the strong electric field always applied across the gap, and they produce an exponential Townsend avalanche whose density increases in the cathode-to-anode direction. The positive ions thus produced drift toward the cathode and some of them are withdrawn through a narrow slit in the cathode and are focused by an ion lens onto the focal plane of a time-of-flight mass analyzer. A draw-out pulse accurately delayed from the photoelectron pulse initiates mass analysis of the ion beam. McAfee and Edelson used drift tube pressures up to 10 torr and, except for four data points for N_4^+ , used an E/p_0 of between 70 and 1000 V/cm-torr. In order to get the four low E/p_0 data points for N_4^+ , they had to modify their drift tube. They added an additional grid to confine the Townsend discharge to a smaller volume and thus to permit a lower electric field in the drift region than that in the discharge region. Their results are shown in Chapter III.

In 1963 Wobshall, Graham and Malone,⁴² measured the thermal energy elastic collision cross section for N_2^+ ions in N_2 by ion cyclotron resonance techniques. This cross section is consistent with a zero-field, reduced mobility for N_2^+ of 1.85. Ionic mass identification is inherent to the ion cyclotron resonance method of investigation.

The Present Work

Because of the discrepancies among existing mobility measurements in nitrogen, the present work had the following objectives:

1. To measure accurately the mobility of each of the four principal ions in nitrogen: N_1^+ , N_2^+ , N_3^+ , and N_4^+ .
2. If possible, to identify the ion or ions involved in the earlier mobility measurements.
3. To determine which ion is most abundant at low pressure and high E/p_0 .
4. To determine which ion is most abundant at high pressure and low E/p_0 .
5. If possible, to obtain evidence clearly supporting or rejecting Varney's 1953 reaction scheme.
6. To obtain information about the mechanism of the creation of N_3^+ and N_4^+ .

The apparatus that has been developed for the present investigation was designed with the specific objective of analyzing ions which have been caused to drift for a known and controllable distance at low energies through a relatively high pressure gas, so that a large and variable number of collisions of the ions with the gas may occur. To accomplish this purpose, a modified Nier-type mass spectrometer was coupled to a drift tube by means of differentially pumped chambers to form a "drift tube mass spectrometer." Great care was taken in the design of the coupling so that the ions of nearly thermal energy coming from the drift tube could negotiate the aperture system in the differentially pumped chambers and so that the ions detected in the spectrometer

would be representative of the ionic population at the exit end of the drift tube. This aspect of the design is discussed at length in Chapter II.

The apparatus used in the present work differs in its source and source supports from that used in the first work of this type performed in this laboratory⁴³. The present apparatus has an electron-bombardment ion source which is movable along the axis of the tube in place of the four fixed crude sources used previously. In addition, many instrumental changes have been made to improve the accuracy of the measurements. Among these changes are numerous improvements of the vacuum system, modifications of the time analyzer to improve its reliability and flexibility, and changes in the McLeod pressure gauge hookup.

The present apparatus has two main drawbacks. The first of these deficiencies is a result of the fact that the apparatus used here is an experimental version of a new type of instrumentation designed specifically for the kind of research reported here. This equipment evolved over several years of experimentation during which almost every component of the apparatus was redesigned and rebuilt at least once. The need for the ability to make significant modifications with comparative ease was anticipated when the construction was initiated, and the decision was made to utilize high-vacuum techniques rather than the ultra-high vacuum techniques already available at that time. No part of the system can be baked, and its base pressure is no lower than 5×10^{-7} torr. Consequently, significant traces of impurity gases are present in the apparatus, and impurity ions are produced in the drift tube in measurable numbers, as expected. Fortunately the resulting impurity

ions are rejected by the mass spectrometer when it is tuned to one of the desired peaks, but effects of the presence of impurities on the mobilities to be measured remain a problem. Recommendations concerning the elimination of this problem in a new version of this apparatus are presented in Chapter V.

The second deficiency of the present apparatus is that the gas pressure is measured with a cold-trapped McLeod gauge. In light of the errors that can be introduced by such a trap (see Appendix A), one would prefer a non-trapped gauge of equivalent absolute accuracy. No such gauge is currently available.

CHAPTER II

EXPERIMENTAL APPARATUS AND METHOD

An overall view of the experimental apparatus is shown in Figure 2. The essential components of the apparatus are shown in Figure 3. The potentials shown are typical of those used during measurements. The components to the left are housed in a cylindrical drift tube; the exit aperture is in one end of the drift tube. The plate containing this aperture, the conical skimmer with its pinhole, and the collimator plate with its slit define two individually pumped chambers which separate the relatively high pressure region of the drift tube from the low pressure region of the mass spectrometer. The ion accelerating electrodes of the spectrometer are shown in the figure. Ions are created in brief bursts by the ionization source, and they drift through the gas under the influence of the axial electric field. Some of the ions that drift along the axis of the tube exit through the apertures and pass into the mass spectrometer where they are mass-analyzed. Electronic equipment counts the ions of a particular mass which reach the detector in the mass spectrometer and sorts them according to their total flight time. A more complete description of this equipment as it existed at an earlier stage of development can be found elsewhere⁴⁴.

The apparatus used in the present work has four great advantages over the mobility apparatus used by earlier experimenters:

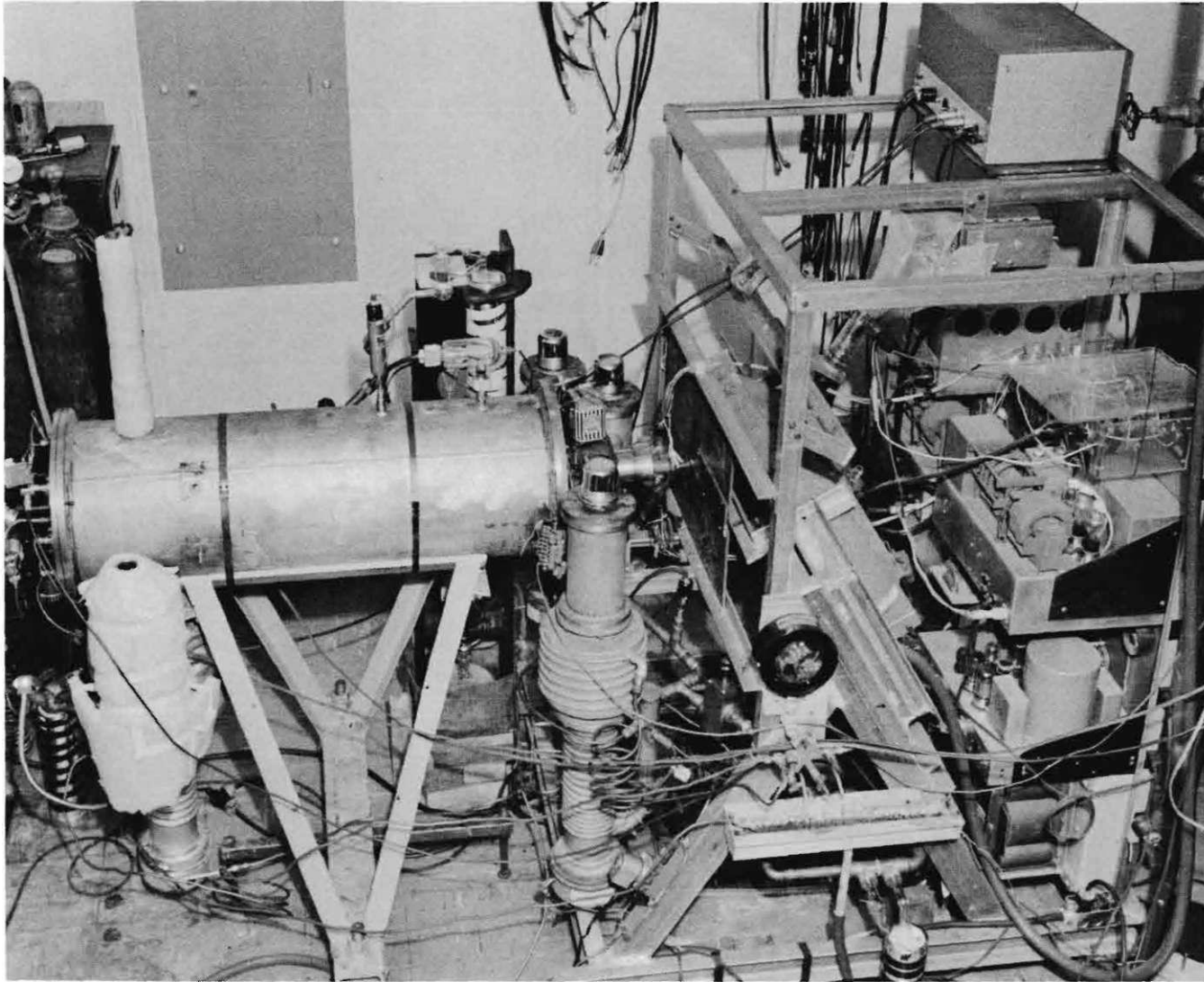


Figure 2. Overall View of the Experimental Apparatus.

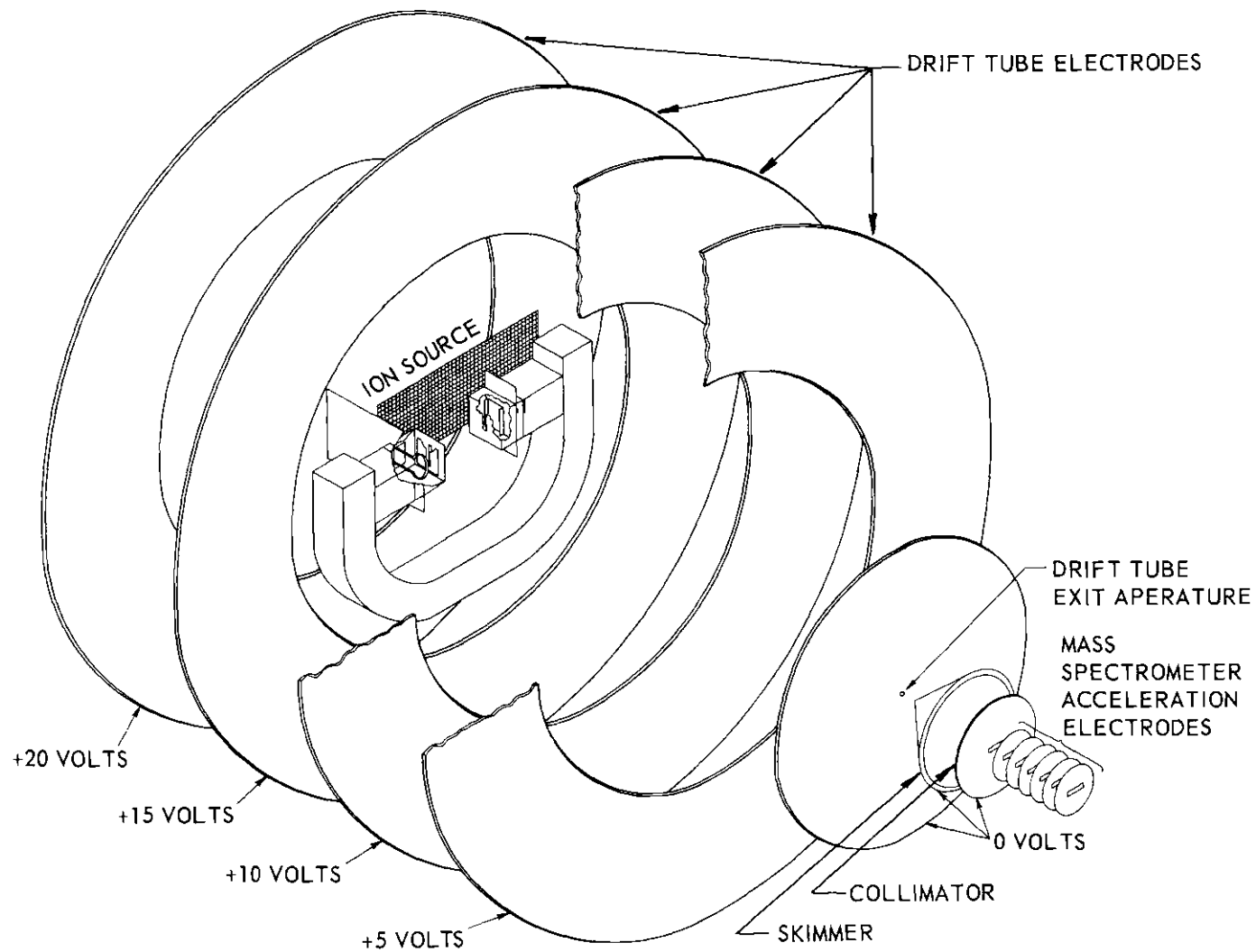


Figure 3. Schematic View of Internal Components of the Apparatus.

1. The ions involved in the mobility measurement which are detected in the mass spectrometer are identified by their charge-to-mass ratio.

2. The ion source position can be varied between extremely wide limits even while the source is in operation. Furthermore, the location of the source is not restricted to a few discrete positions, but rather can be changed continuously.

3. The available drift distance is 34 cm, several times as long as the distance available in any other currently used mobility apparatus. This feature, combined with the movable source arrangement, permits runs to be made at two widely separated positions. One can then take a difference of the apparent mean drift times to eliminate end effects. The long drift space permits accurate measurements of drift distance differences and drift field intensity E . Because the ions are in the tube so long, the timing of the experiment can be performed by conventional microsecond circuitry.

4. The mass spectrometer used here is equipped with an ion multiplier detector, which permits the gathering of data even though the signal may be extremely small. (In this work, five ions per minute was the practical lower limit.) This capability permits data to be taken at quite low E/p_0 .

Drift Field and Ion Source

A static, nearly uniform electric drift field is established by seven drift field electrodes mounted on a stainless steel rack in the manner shown in Figure 4. These electrodes are each connected via a shielded wire to one pin of an eight-pin kovar seal in the side of the

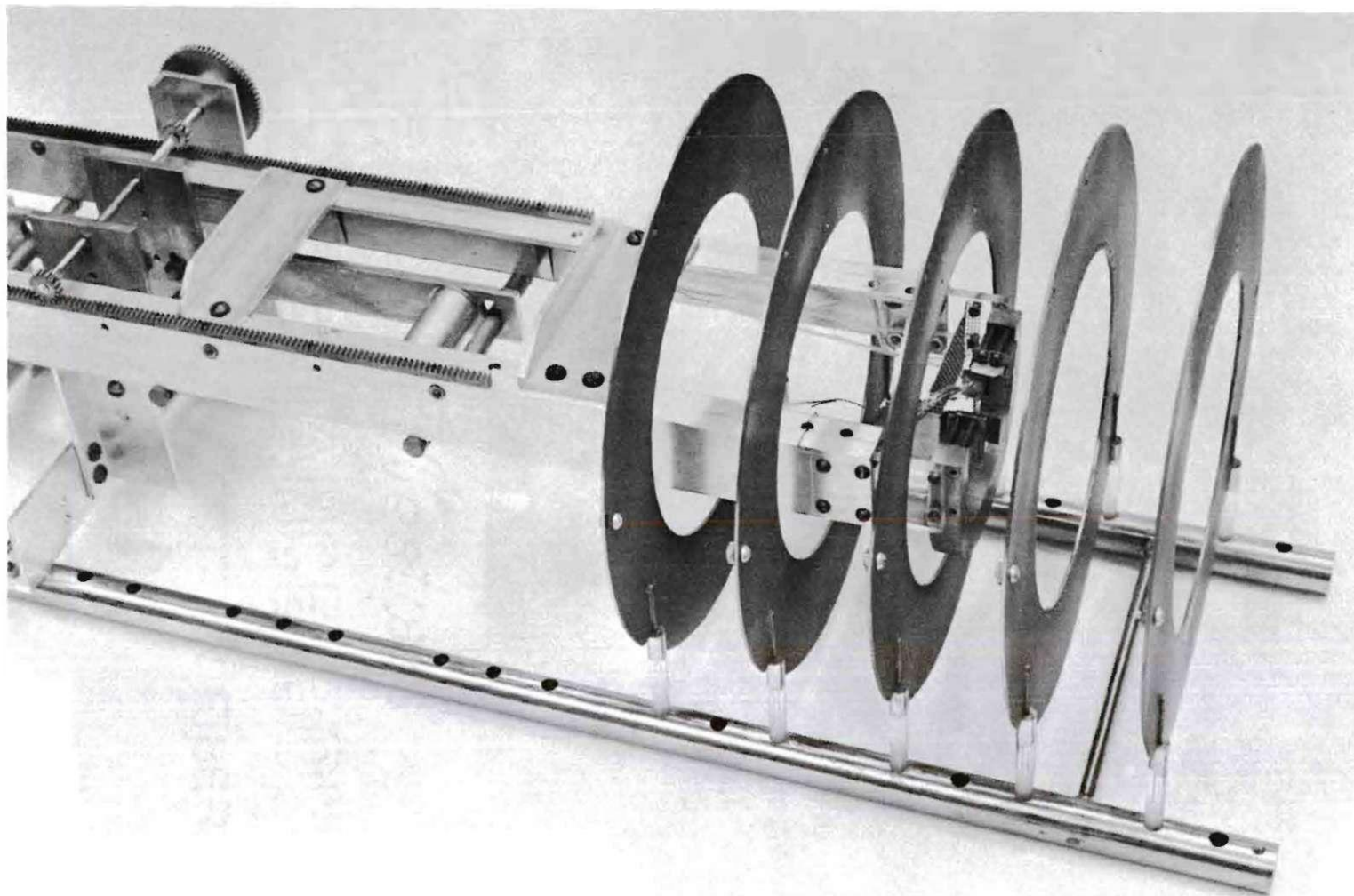


Figure 4. View of Source, Source Supporting Structure, and Drift Field Electrodes.

drift tube. The total voltage of the drift field is distributed to the electrodes from a string of 1.81K-ohm one-percent precision resistors mounted on the kovar seal outside the drift tube. The drift voltage is supplied by a Universal Electronics Regulated Power Supply, Model 300B, and is monitored with a Triplet volt-ohm meter, Model 630-PLK. Near the drift electrode which is closest to the exit aperture is suspended a very fine chromel-alumel thermocouple for determining the temperature of the gas in the drift region. Its reference junction is the kovar seal on which it is mounted. The temperature of the gas has been measured to be about 305° K during a run.

The electron-bombardment ion source is shown in Figures 4 and 5. The electrical design of the ion source can be seen in the wiring diagram for the source, Figure 6. The source consists in part of a non-magnetic stainless steel box mounted on each pole of a magnet. The magnet, whose function is to confine the ionization-producing electrons to the intended ionization region, was designed to maintain a flux density of 100 gauss at the center of its 1-1/2-in. gap⁴⁵. In one box a thoriated-iridium filament is mounted 1/2 mm behind the control plate. The control plate, which functions like the grid of a triode vacuum tube, contains a 1-1/2-mm by 1.0-cm vertical slit. One millimeter in front of the control plate slit is the 0.7-mm by 1.0-cm vertical exit slit. The control plate is mounted on the plate containing the exit slit with all-glass "rivits." The other box has a 3-mm by 1.0-cm vertical collector slit backed by a collector cup. This box collects all the electrons which have traversed the ionization space. This space contains no physical objects, but is exposed to the drift tube gas, the magnetic

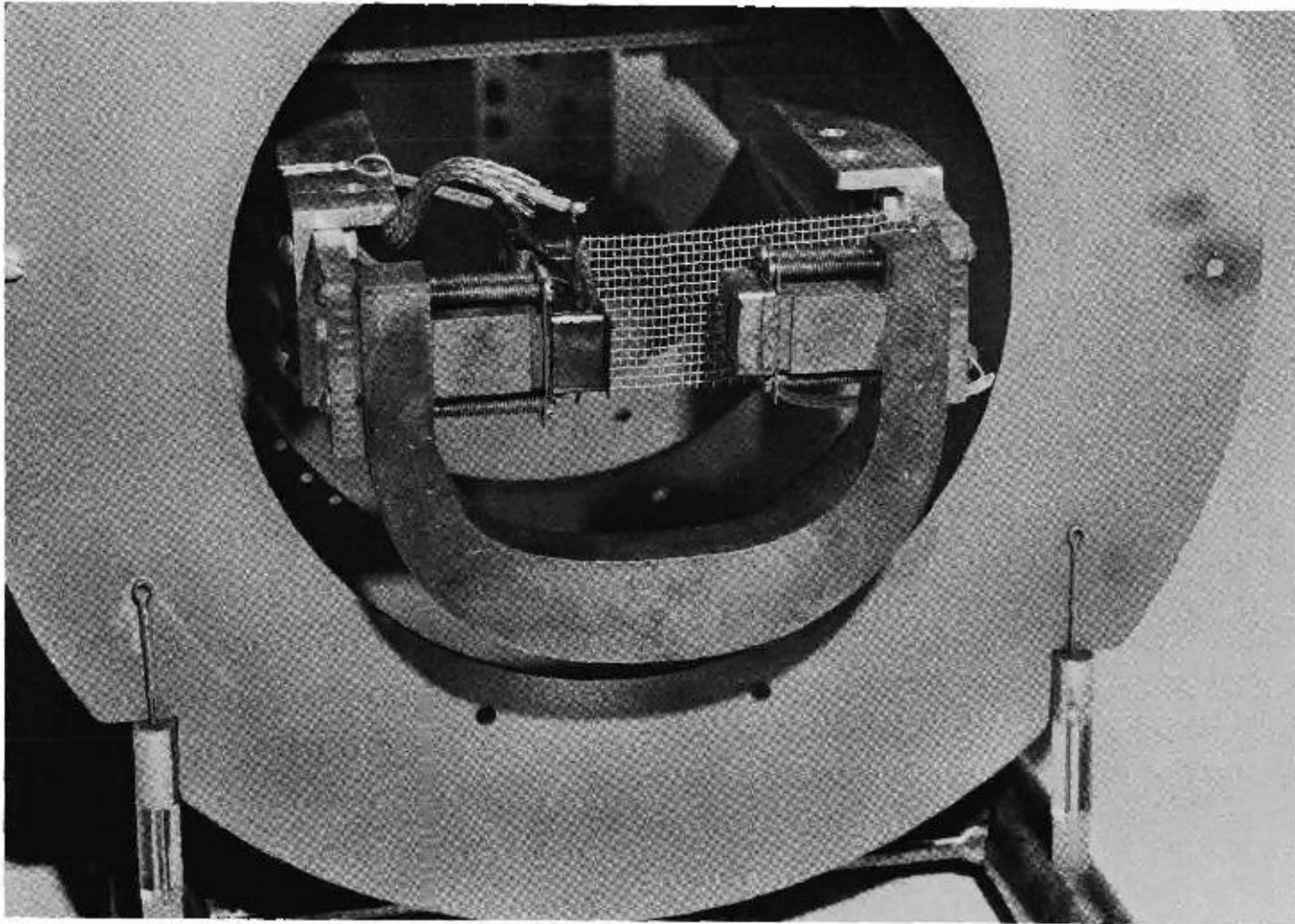


Figure 5. View of Source.

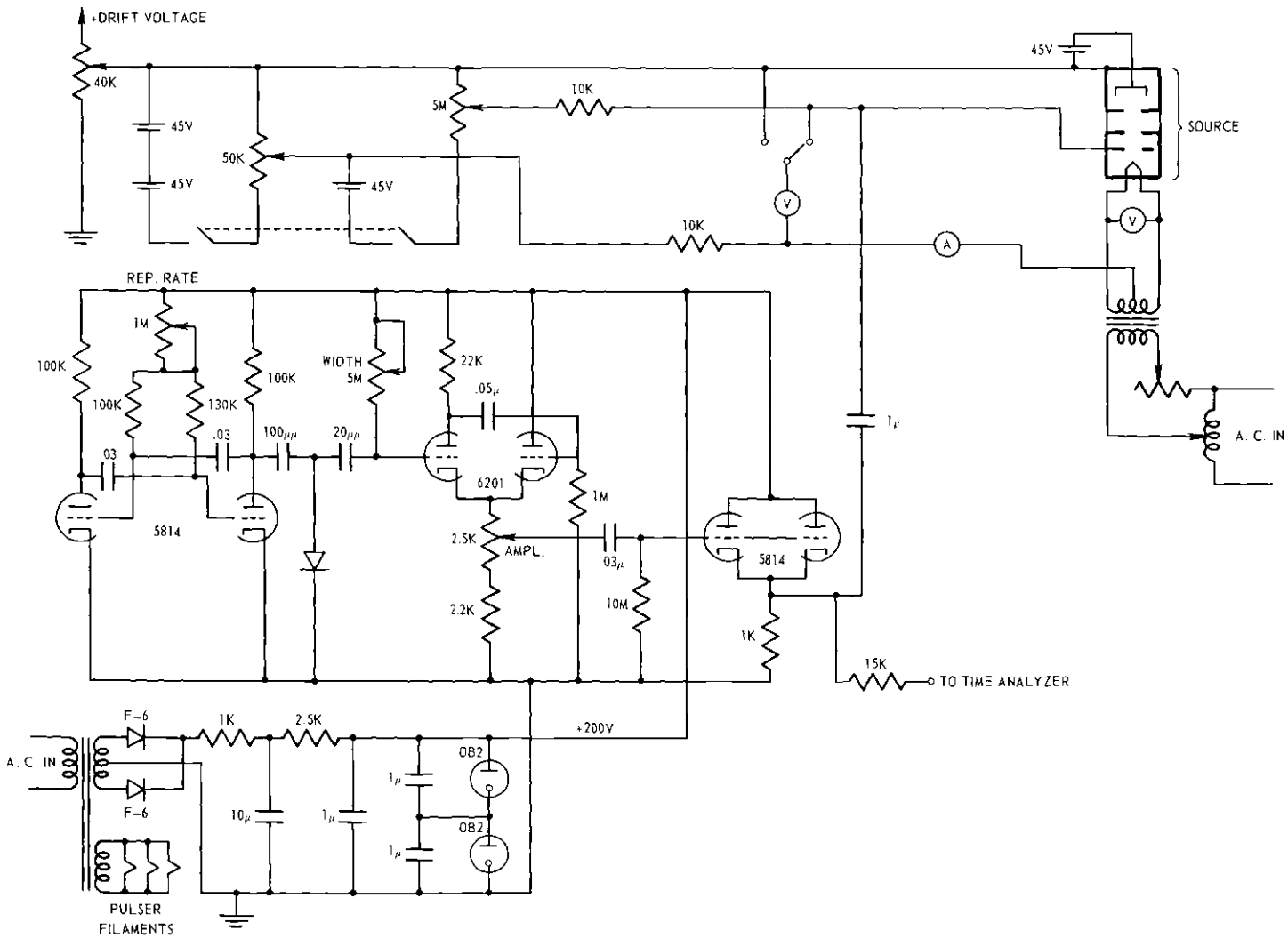


Figure 6. Source Circuitry.

field of the magnet, and the electric drift field. The source frame is maintained at the potential of the drift field at the source position.

Both the control plate slit-exit slit combination and the collector slit are adjustable horizontally for the purpose of alignment. The collector slit is adjusted to maximize the current to the collector box. It is found experimentally that the best alignment possible can be obtained visually by using the clearly visible purple glow resulting from the excitation of the gas in the ionization space.

To insure that the ions are formed in an electric field as nearly as possible identical to the drift field, there is a piece of wire screen (a "repeller") mounted behind the source whose dc potential is set from outside the drift tube. The screen is located 1-1/2 cm behind the slits so that a 1-1/2-volt dry cell produces a one volt per centimeter field in the region of ionization.

The source is mounted on plexiglass struts which attach to an aluminum frame (Figure 4). The aluminum frame rolls on brass rollers supported by a stainless steel and aluminum structure. This structure bolts to the stainless steel rack which holds the drift electrodes. The aluminum frame is moved back and forward by a rack and gear arrangement which can be seen in the figure. The driving gear is attached to a 3/8-in. brass shaft which passes through an "O" ring seal to the outside of the drift tube. Thus the source can be propelled backward or forward from outside the drift tube even while the source is in operation.

Electrical leads to the source elements are insulated with loose teflon spaghetti and are strapped inside the aluminum frame. The leads

which conduct no appreciable current are attached to kovar seals in the back plate of the drift tube by hand-wound springs. These springs are convenient connections to the movable frame, but they do have non-zero resistance. The filament leads, which must conduct several amperes, are made of large diameter stranded wire, insulated and shielded.

The wiring for the source is shown in Figure 6. The top unit of the wiring provides filament power and the necessary dc voltages for the source. The design of the source and its circuitry was strongly influenced by reference 46.

The second two units of the wiring are the pulser and its power supply. The pulser generates 45-V positive, square pulses of 20- μ sec duration and supplies them to the source control plate and time analyzer at a rate which can be varied from 400 to 13,000 pulses per second. When one turns the pulser on, one also changes the dc potential of the control plate from the potential of the filament to a potential 45-V negative with respect to it, which biases off the electron beam. Thus a 45 V positive pulse applied to the control plate permits a burst of electrons to enter the ionization region.

Gas Handling System

The nitrogen used in this experiment was prepurified grade and obtained from the Matheson Company. It flowed first into a high pressure regulator and then to a vacuum regulator set at between 100 torr and 700 torr. Both these regulators were enclosed in a plastic bag, which is kept inflated with a steady flow of dry nitrogen gas at a pressure of one or two pounds per square inch. This arrangement virtually eliminated

the presence of oxygen that otherwise diffused through the rubber diaphragms of the regulators and appeared in the mass spectra as mass 30 (NO^+) and mass 32 (O_2^+). The gas then entered the gas feed line, a 40-foot length of 1/4-in. copper tubing. Most of the length of this tubing is wound into a tight coil which was immersed in liquid nitrogen during a run. The feed pressure of less than one atmosphere permitted the use of liquid nitrogen in the trap without danger of condensing nitrogen in the line. The gas was metered into the drift tube through an Edwards High Vacuum Ltd. needle valve. Between the needle valve and the drift tube is a cut-off valve, so the gas could be shut off to the drift tube without disturbing the setting of the Edwards valve.

The drift tube is pumped between runs by a 4-in. CEC MCF-300 oil diffusion pump. To minimize backstreaming of pump oil into the drift tube, the pump is baffled first by an air-cooled optically-dense chevron baffle, and second by a similar, but liquid nitrogen-cooled, CEC BCR-61 baffle. The second baffle is supplied with liquid nitrogen from a reservoir constructed from a two quart Stanley all-steel vacuum bottle. The reservoir holds a one hour supply of liquid nitrogen. The pump is backed by a Welch 1402-B mechanical pump identical to both of the other mechanical pumps used on this apparatus.

During regular operation the gate valve between the drift tube and its pump is closed. Some gas flows out of the 1/32-in. diameter exit aperture shown in Figure 3. The chamber into which it flows is pumped by a 4-in. CEC MCF-300 oil diffusion pump. Since the pressure in this chamber has been measured to be a factor of 330 lower than that in the drift tube, the conductance of the exit aperture can be used to calculate

that the net pumping speed in the chamber is 33 liters per second. For example, with 100 μ of nitrogen in the tube, the pressure at the top plate of the first chamber is 3×10^{-4} torr. Thus the molecules and ions fan out past the exit aperture into molecular flow (see Appendix C).

Located in the tip of the conical skimmer 1.5 cm behind the exit aperture is a second pinhole of the same diameter cut in a cone-shaped piece of non-magnetic stainless steel. Both of these apertures were made as large as practicable to minimize the effect of grazing collisions between ions and the aperture edges. Behind the skimmer is a 1/16-in. by 1/2-in. collimator leading to the mass spectrometer ion accelerating electrodes. The space between the skimmer and collimator is pumped by a 2-in. CEC MCF-60 oil diffusion pump, and its pressure is typically 3×10^{-5} torr. The mass spectrometer tube is also pumped by a 2-in. CEC MCF-60 oil diffusion pump. The pressure in the tube is typically 3×10^{-6} torr or lower. The pumps on the two chambers and the tube are all baffled by water-cooled baffles and are liquid-nitrogen-trapped by traps constructed from 1 quart Stanley all-steel vacuum bottles. To retard oil accumulation in the chambers, these diffusion pumps are never operated without liquid nitrogen in the traps, and butterfly valves between the chambers and traps are closed when the traps are warmed.

Ideally, the ions should not be accelerated in a region of continuum flow. However, a one-volt positive potential with respect to the grounded skimmer was placed on the exit aperture plate during some of the drift velocity measurements to accelerate and focus the ions somewhat in the first chamber. This potential increased the current intensity to the mass spectrometer and thus the signal-to-noise ratio of the

experiment. Only one volt was used so that collisions in this chamber would be as much like collisions in the drift tube as possible. Any other weak electrostatic or magnetic field can deflect the ion stream from its intended course. To avoid the production of spurious electric fields, and differentially pumped chambers are machined into a single block of stainless steel and their interiors are gold electroplated. To shield the ions in this region from the field of the spectrometer magnet and other magnetic fields a soft iron plate is mounted between the spectrometer magnet and the chambers. Moreover, the outside of the chambers is wrapped with several layers of high-permeability magnetic-shielding foil. This combination of shielding lowers the magnet field inside the chambers to no more than one gauss.

It is found that even with the extensive trapping of pump oil vapors, the exit plate and skimmer must be removed and degreased every few months. When this is done, a large increase in transmission efficiency is noticed. Apparently even a thin layer of pump oil can accumulate enough charge to deflect the thermal ions from their intended trajectory through the apertures into the mass spectrometer.⁴⁷

The transmission of the exit plate and skimmer combination was measured on one occasion just after these components had been degreased. With all the plates at ground potential, it was found that under conditions such that 4.9×10^{-8} A could be collected on the drift tube end plate, a current of 3.4×10^{-12} A could be collected on a plate hung into the first chamber behind the end plate, and 1×10^{-14} A could be collected on a plate hung into the second chamber behind the skimmer. With the end plate at a potential of 1.5 V with respect to the grounded

skimmer, it was found that under conditions such that 3.5×10^{-8} A could be collected on the drift tube end plate, a current of 3.5×10^{-12} A could be collected in the first chamber, and 3.5×10^{-14} A could be collected in the second chamber. These intensity losses combine with a similar intensity loss (about a factor of 5,000) between the second chamber and the detector of the mass spectrometer to make counting of the individual ions absolutely necessary.

The pressure in each of the forelines is monitored with Veeco thermocouple gauges. During pumpdown the pressure in the mass spectrometer tube at the ion multiplier and the pressure in the drift tube are checked with Veeco ionization gauges, type RG-75, used with a Veeco vacuum gauge, Model RG-31A. During runs, the drift tube pressure is measured by a CEC McLeod Gauge, type GM100A. To protect the drift tube from mercury vapor and the McLeod gauge from condensibles in the tube, the gauge hookup includes a cold trap, a valve on the drift tube, and a stopcock between the trap and valve. This trap is designed to prevent any error from being introduced by thermal transpiration⁴⁸ (see also Appendix A), which effect is important at the pressures used in this experiment. The valve was never opened unless the trap was iced with liquid nitrogen. Each of the vacuum gauges is near enough to the exit end of the drift tube to insure that the readings are representative of the pressure in the active drift region.

The McLeod gauge must be removed from the drift tube to enable the drift tube to be opened at the source end. At these times it proved convenient to have the stopcock mentioned above. One could close it,

remove the connecting pipe to the drift tube valve, and remove the gauge without bringing it up to atmospheric pressure, thus minimizing the introduction of impurities into the gauge and its cold trap.

The drift tube contains a large, stainless steel trap constructed from a 1-qt. Stanley all-steel vacuum bottle. Refrigerating this trap produces a drop in background pressure of at least 40 per cent and greatly reduces the impurity mass peaks, which otherwise can be seen at nearly every mass number from 12 to 60.

Mass Spectrometer and Counting Equipment

The mass spectrometer is essentially a Nier⁴⁹ 60⁰ type, except that it has no internal ion source. It has a resolving power of about 75. The width of the exit slit of the mass spectrometer was not made much greater than the width of the focused ion beam at the slit, so that the mass-peak heights cannot be taken as quantitative measures of ion numbers in the ion beam; the width of the slit was not made much less than the width of the beam, so that neither can mass-peak areas be taken as quantitative measures. For this work, the mass-peak heights were used as qualitative measures of intensity. The accelerating potential for the incoming ions is provided by a Beva Laboratory Model 301, 5.1-kV power supply. It has been modified to provide a linear scanning of voltage at any of nine different speeds. The ions are detected with a 12-stage DuMont multiplier with silver-magnesium dynodes, the multiplier being used as a discrete particle counter and not as a current-measuring device. The counting efficiency of this multiplier has never been able to be measured accurately, but it is estimated to be from 10 to 50 per cent.

The current to the mass spectrometer's electromagnet is supplied and controlled by a Process and Instrument Company current supply. The magnetic field was at first measured with a Harvey-Wells NMR gaussmeter to locate the array of mass peaks normally observed in nitrogen. Subsequently the field strength, when needed, has been calculated from the accelerating voltage needed for a particular mass peak.

The output of the ion multiplier leads to a preamplifier and linear amplifier, Baird Atomic Models 219A and 218. The latter instrument contains an integral pulse height discriminator which is used to reject virtually all noise pulses generated in the multiplier, preamplifier, or amplifier. The maximum number of such noise counts tolerated is about four per minute. The shaped output of this discriminator has been attenuated by a factor of ten and is connected to a Nuclear Chicago Model 182 scalar which counts the pulses.

The scalar's internal amplifier supplies shaped pulses to the detector input of an Eldorado Electronics, System 1500, twenty-channel time analyzer. The same pulser that operates the ion source provides "triggering" pulses for the time analyzer, which start the timing circuits of the analyzer. The standard available channel widths provided on the analyzer were 10 μ sec, 100 μ sec, 1 msec, 10 msec, and 100 msec. The analyzer has been modified, however, to provide additional channel widths of 30 μ sec and 400 μ sec.

Experimental Techniques

Overnight and on weekends and holidays the equipment was left almost completely turned off. The gate valve below the drift tube was

closed, and the equipment was pumped only by the mechanical pump below the differentially pumped chambers and mass spectrometer. The entire working volume of the McLeod gauge was left filled with mercury so that impurities which evolved from the warming cold trap could not contaminate the surface of the glass. The stopcock was left closed so that the impurities could not enter the drift tube.

On a day when drift velocities were to be measured, the first action in the morning was the opening of the gate valve below the drift tube and the direct diffusion pumping of the drift tube, the differentially pumped chambers, and the mass spectrometer to effect as much cleansing as possible. A pressure of about 5×10^{-7} torr was reached before proceeding with the run. During the pumping, the McLeod gauge was opened to the drift tube and its capillaries heated with a hot air gun to drive off adsorbed condensibles. Also the ion source filament was turned on to allow it to degas thoroughly. Near the end of this pumping, prepurified nitrogen was bled into the drift tube to establish an equilibrium pressure of about 5×10^{-4} torr. This action noticeably decreased the impurity level in the run following. The gate valve was then closed, and the Edwards valve was adjusted to achieve the equilibrium pressure desired to the drift tube. This pressure was monitored with the Pirani gauge until equilibrium was established, and was then measured with the McLeod gauge. An attempt was made to maintain this same pressure all day, and the pressure was checked frequently with the McLeod gauge.

As soon as the pressure had become stabilized, the drift voltage power supply and the source dc power were turned on, and the desired

mass peak was located by sweeping the mass spectrometer ion acceleration voltage. With the mass spectrometer tuned to the top of the desired mass peak, the pulser was turned on and the arrival times of the incoming ions were sorted by the time analyzer. From the distribution of the arrival times, a mean drift time (see Appendix B) was calculated for the ions of the desired mass for the combination of drift field, pressure, and source position chosen for that run. Then the source position was changed, and another mean drift time was determined. The difference between these times was divided into the distance the source had been moved to determine the drift velocity of the ion for that value of E/p_0 . The drift field alone was then varied to change to other values of E/p_0 .

CHAPTER III

RESULTS

Factors Affecting the Accuracy of the Measurements

The primary factors affecting the accuracy of the experimental measurements were the presence of impurities; uncertainties in the measurement of the reduced pressure, drift distance, drift field and drift time; source effects; and the transmission of the differentially pumped chambers.

The Presence of Impurities

At an early stage of development of this equipment the presence of many impurities could be detected with the mass spectrometer. When the drift tube was filled with nitrogen, in addition to the nitrogen peaks [mass 14 (N_1^+), mass 28 (N_2^+), mass 42 (N_3^+) and mass 56 (N_4^+)] ions with the following masses were seen: 29 (N_2H^+), 19 (H_3O^+), 18(H_2O^+ or NH_4^+)⁵⁰, 30 (NO^+), and 32 (O_2^+).

A change to the use of liquid nitrogen instead of dry ice and acetone to trap impurities in the gas feed line virtually eliminated the ions of mass 19 and reduced the number of ions of mass 18. The impurity ions of mass 32 and 30 virtually vanished when the gas regulators were enclosed in an atmosphere of dry nitrogen. Since that time, the reappearance of O_2^+ has been the most sensitive indication of a vacuum leak in the drift tube.

At the time the data to be described were taken there were still some mass 29 ions and some mass 18 ions present. These remaining

impurity ions could not be eliminated by extended pumping or "flushing" of the drift tube. They probably resulted from reactions of the nitrogen gas with traces of water vapor not condensed on the main drift tube cold trap or with traces of pump oil or other hydrocarbons on the inside walls of the drift tube. Further reduction in the impurity level did not seem possible without baking the drift tube, and baking was not feasible because of various constructional features of the drift tube described earlier.

In general, impurities could affect these measurements of nitrogen ion drift velocities if there were reactions forming the ions under investigation from impurity ions, for then part of the drift time measured would refer to the drift of the impurity ion. Fortunately no reaction forming nitrogen ions from the two remaining impurity ions has been seriously proposed. Therefore, the measurements of the nitrogen ion drift velocities are not believed to be significantly affected by the remaining impurities.

The Four Physical Measurements

The Pressure Measurement. By far the most uncertain of the physical measurements was that of the pressure. The pressure was measured with a liquid-nitrogen-trapped McLeod Gauge, CEC Mod. GM100A. This gauge comes from the manufacturer with no warning of the dangers involved in cold-trapping the gauge (see Appendix A), a step which is necessary to keep mercury vapor out of the drift tube.

During the present investigations the cold trap was changed from one that was arbitrarily sized to one designed to minimize the effects of thermal transpiration. A definite drop was noticed in the drift

velocity data immediately following this change. Although no exact record was made of the amount the data were shifted by this change, since certain other changes were made at the same time, the drop was between five and ten per cent. A drop of this magnitude would be expected from the change effected in the trap.⁴⁸

Published analyses^{51,52,53,54} of the Gaede mercury pumping effect indicate that in the pressure range of the present work (50 μ to 200 μ) this effect produces an error in the pressure measurement of less than two per cent. Anyone using a trapped McLeod gauge should be alert to the literature, however, for later findings concerning this effect.

Several routine procedures were followed to help add consistency to the readings of the McLeod gauge. First, the gauge was diffusion pumped and heated with a hot air gun for an hour before each day's data taking. Second, at least once a week the mercury was raised in the gauge while it was at high vacuum (about 10^{-6} torr). At a number of points the levels of mercury in the closed and open capillaries were compared to verify that the capillaries were equally clean. (If they were, the levels would be the same up to a point very near the top of the gauge. If not, one mercury level would lead the other.) If the capillaries were not equally clean, an appropriate calibration factor was measured. This factor was always less than two per cent. Third, since the quadratic pressure scale used to read pressures from 0 μ to 100 μ was much longer than the 0 μ to 100 μ portion of the next less sensitive scale, the quadratic scale was used as the standard when these two scales disagreed. This disagreement was always less than five per cent. Fourth, the capillaries were tapped vigorously as one came up to a

reading. Fifth, it was found that if one permitted the mercury to rise past the point for reading, the reading could not be recovered simply. Readings which had been overrun were found to be in error by several per cent and were not believed.

The analysis of these data required the use of the reduced pressure, defined by Equation (3). For this reason the temperature of the gas was measured, as has been described in Chapter II. An average temperature of 305°K was measured; the deviation from this temperature was always less than two per cent.

Overall, even with the precautions that were taken in reading the McLeod gauge, it is still believed that the measurement of the reduced pressure may have been in error by five or six per cent.

The Time Measurement. The next most difficult measurement was that of the time. Fortunately, the times to be measured were longer than $50\ \mu\text{ sec}$, and conventional tube-type circuits could be used.

The scaling stages of the time analyzer that was used employ Sylvania 7155 decade scaling tubes. The standard scaling circuits of the analyzer were unable to drive these tubes dependably, but suitable modifications were made on these circuits to eliminate the difficulty.

The time base of the time analyzer is a 100 kilocycle oscillator. The accuracy of the output of this oscillator was checked by counting the output pulses for one minute. The total error in this count was less than 0.3 per cent. The timing of the experiment was checked independently by displaying with a Tektronix Model 545 Oscilloscope having a Type 53/54K plug-in amplifier the pulse to the source and the incoming pulses from the ion multiplier. Time exposures of these displays were

made with a Polaroid oscilloscope camera. Comparison of the photographs with data taken immediately before or after on the time analyzer showed no significant difference in drift time differences.

The scheme of using only differences of mean drift times made it unnecessary to evaluate any of the short but constant time lags in the timing circuits. A rather involved daily testing routine was developed for the time analyzer to insure that this relatively complex instrument was functioning properly. It is felt that the timing of the measurements was not in error from instrumental effects by more than two per cent.

The Drift Distance and Drift Field Measurement. The easiest physical measurements to make were those of drift distance and drift field. The source was moved by a rack and gear arrangement mentioned earlier. Small errors in the positioning of the source could cause errors in individual data points, but these errors should have averaged out. The absolute accuracy of the drift distance measurement, then, depended only on the accuracy of the machines that cut the racks and gears, and this is believed to be less than one per cent in error. The drift field was established by drift electrodes whose separation was accurately determined by their mounts. The voltage-dividing string of resistors was accurate to one per cent. The total drift voltage was monitored by a new Triplet volt-ohm meter whose readings were accurate to two or three per cent. Therefore, measurement of the drift field between the two source positions that were used should have been accurate to three or four per cent.

The Over All Accuracy. Taking into account all the factors that have been enumerated, one is led to believe that the absolute accuracy of the data to be presented should be plus or minus seven per cent ($\pm 7\%$).

Source Effects

Non-Zero Pulse Width. The output of ions from the source was not an ideal three dimensional delta function in space and time, for which the configuration of the ions at any later time or location can be described in closed algebraic form (see Appendix B). A 20- μ sec pulse duration for the source control plate was selected as a good compromise between intensity and time resolution. The 20- μ sec pulse ideally produced an initially uniform distribution of ions one cm high (the electron exit slit height), 2-1/4-cm wide (the source gap dimension), and about one cm deep (20 μ sec times 4×10^4 cm/sec, a typical drift velocity). The non-zero time width of this pulse broadened the peak width beyond the expected value (see Appendix B), but the use of mean drift time differences nevertheless permitted relatively accurate drift velocity calculations. From single, undifferenced runs one would eventually hope to get a diffusion coefficient along with the corresponding mobility. The non-zero pulse width and other factors have prevented this so far, however.

Mutual Repulsion. It was quite easy to increase the ion output density from the source above its normal level and observe the effects of mutual repulsion among the ions. One effect of mutual repulsion is the broadening of the peaks in the arrival time spectrum. In the present apparatus, the peaks became noticeably broadened when the electron

emission of the filament during a pulse was raised above the normal value of about three microamperes. A calculation of the approximate charge density just after the pulse showed that at an electron current of three microamperes the ionic number density n_i in the ionization region was almost 10^8 ions/cm³. Mutual repulsion is expected to manifest itself when $n_i \gtrsim 10^8/\text{cm}^3$,⁵⁵ so that this observation was not surprising.

In addition to an overall spreading of the burst of ions by mutual repulsion, however, there was a definite spreading of the burst in the direction of the drift field. That is, the mean drift time for the burst was reduced.

The Transmission of the Differentially Pumped Chambers

The transmission of the differentially pumped chambers was the most erratic feature of the present apparatus. The plates containing the apertures had to have a clean, bright coat of gold for transmission to be a maximum. Since oil diffusion pumps were used, a new gold coating did not fulfill its intended function forever, and the plates had to be removed and degreased periodically. The gold coat was renewed when its quality became doubtful.

The usual indication that degreasing of the plates was necessary was that the transmission of the differentially pumped chambers was a rapidly increasing function of time when the source was operated continuously and a slowly decreasing function of time (with a time constant of one minute to several hours) when the source was operated in the pulsed mode. One could infer that if the plates were slightly coated with pump oil, the maximum transmission could be obtained only if the

oily surfaces become charged with positive ions collected from the ion stream.

The several attempts that were made to measure the times of transmission of the various ions through the chambers have not succeeded because the times varied too much to be precisely determined. Fortunately, mean drift time differencing made this knowledge unnecessary, at least as far as the measurement of drift velocities was concerned.

It is believed that relatively few of the ions that were mass-identified and counted had undergone reactions in the differentially pumped chambers. The arrival time spectra (Figures 8 and 9) show some fine details that suggest transitions from one ion type to another near or in the chambers, but the percentages of ions undergoing such changes must have been small. It is thought that the chambers had no net effect on the absolute accuracy of the data.

The Measurements

The principal results of the present experiment are shown in Figures 7, 8, and 9. In Figure 7, the solid lines superimposed on the data for N_1^+ , N_2^+ , and N_4^+ are the best-fitting straight lines with a slope of unity. The solid line superimposed on the data for N_3^+ is the best-fitting straight line and does not have unit slope. The three dashed lines indicate the direction and the extent that the data for N_3^+ , N_4^+ , and N_2^+ are scattered for the indicated pressure regions (see the key in the figure). The implied zero-field, reduced mobilities for N_1^+ , N_4^+ , and N_2^+ can be obtained directly from the figure; at the value of E/p_0 indicated by the arrows the ordinates of the data can be

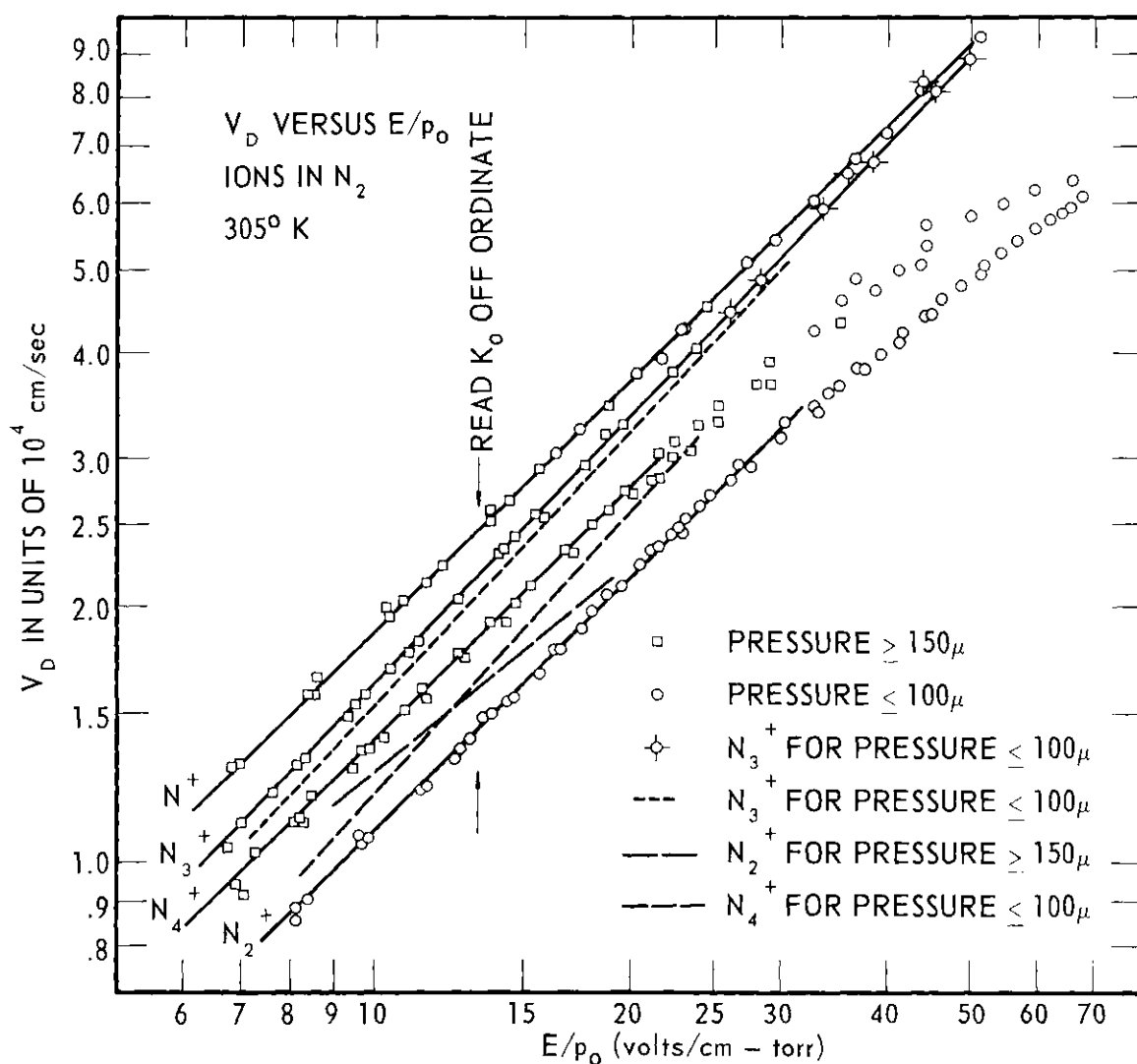


Figure 7. Drift Velocity Data for Mass-Identified Ions in Nitrogen.

Note: The symbols denote the experimental data of Keller, Martin, and McDaniel (1965). The solid lines superimposed on the data for N_1^+ , N_2^+ , and N_4^+ are the best fitting straight lines with a slope of unity. The solid line superimposed on the data for N_3^+ is the best fitting straight line and does not have unit slope. The three dashed lines indicate the direction and the extent that the data for N_3^+ , N_4^+ and N_2^+ are scattered for the indicated pressure regions (see the key in the figure).

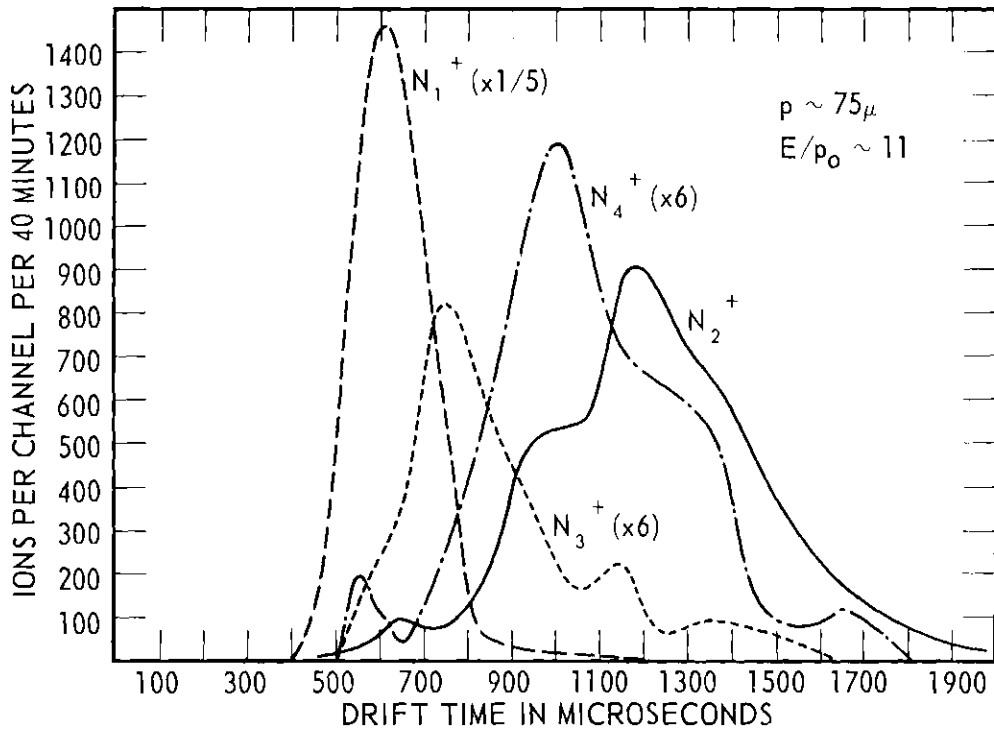
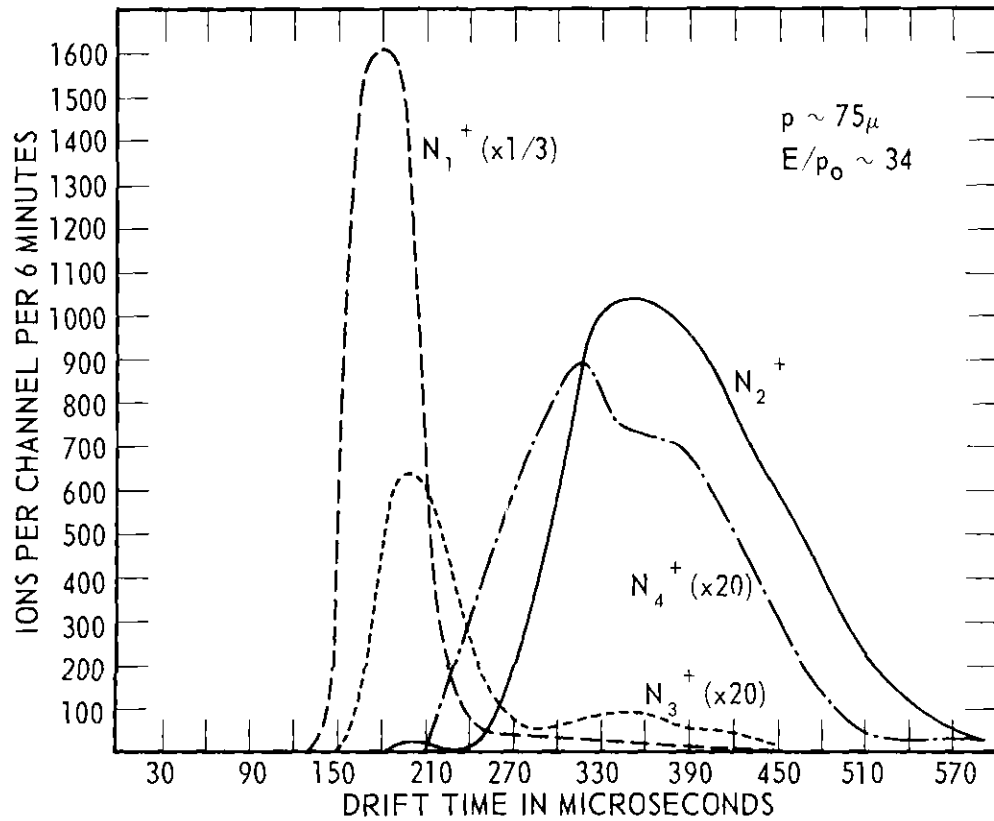


Figure 8. Arrival-Time Spectra - Low Pressure.

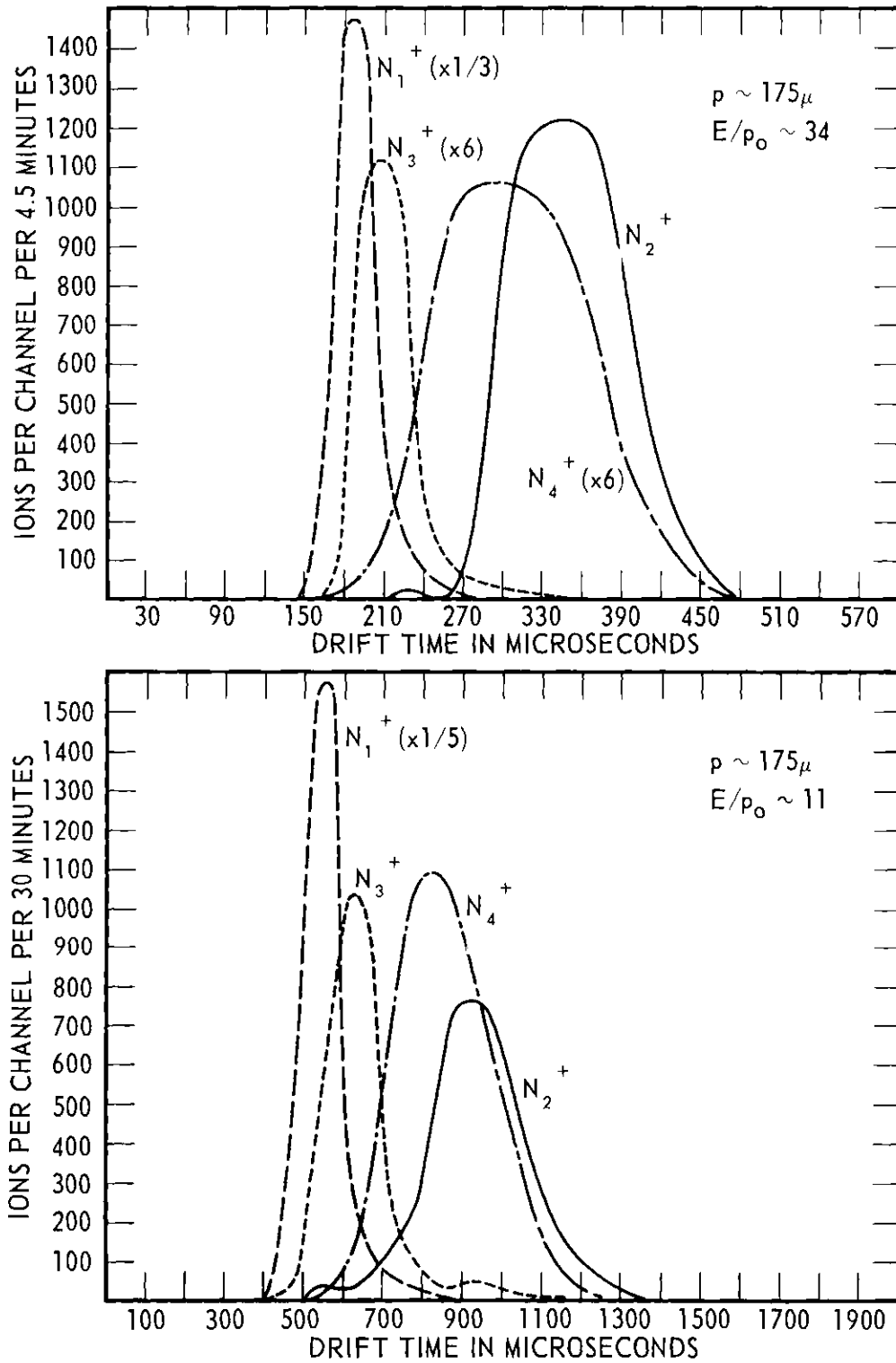


Figure 9. Arrival-Time Spectra - High Pressure.

read directly as the zero-field, reduced mobilities in units of $\text{cm}^2/\text{V-sec}$. The measured drift velocities are compared with the latest, unpublished data of Saporoschenko⁵⁶ and with the data of McAfee and Edelson⁴² in Figures 10 and 11. The drift velocities are compared with the measurements of a number of other experimenters in Figure 12. In these three figures, the present results are labeled "Keller, Martin, and McDaniel (1965)."

The Drift Velocity Measurements

The linearity and the unit slope of the log-log plots of v_d vs E/p_0 at low E/p_0 for three ions in Figure 11 imply that the energy of most of the ions in the drift tube at low E/p_0 was nearly thermal. An earlier retarding-potential measurement in the present investigation had shown that at E/p_0 of about 10, only 33 per cent of the ions counted had an energy greater than 0.5 eV, 6 per cent greater than 1.0 eV, and 0.55 per cent greater than 1.5 eV. The very small scatter of the data for N_1^+ demonstrates the reproducibility of many instrumental measurements, including the pressure measurements. The data clearly show the advantage of an experimental arrangement having the ability to yield "low" E/p_0 results, in this experiment results below E/p_0 of 20 volts/cm-torr. The linear, unit slope plots of v_d in this E/p_0 region allow the zero-field mobilities to be inferred from the drift velocity data without resort to extrapolation, which may be misleading if the measurements do not reach low E/p_0 .

The small scatter of the drift velocity data for N_1^+ shown in Figure 7, and the sharpness and lack of structure of the arrival time spectra for N_1^+ shown in Figures 8 and 9, are important. These facts suggest that the N_1^+ ions that were seen were formed only at the source and not from other ions by collisions in the drift tube. Therefore, a

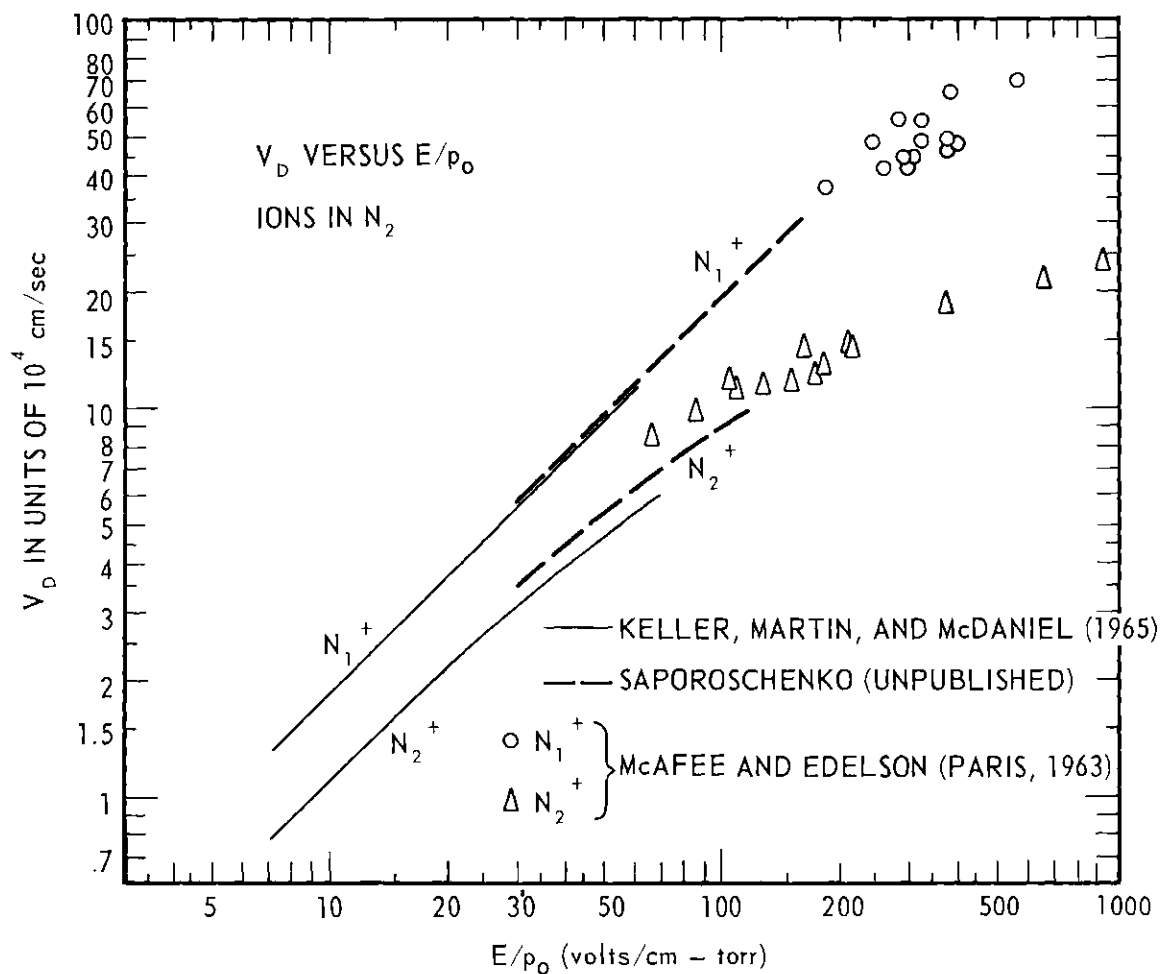


Figure 10. Comparison of Msss-Analyzed Drift Velocity Data - N_1^+ and N_2^+ .

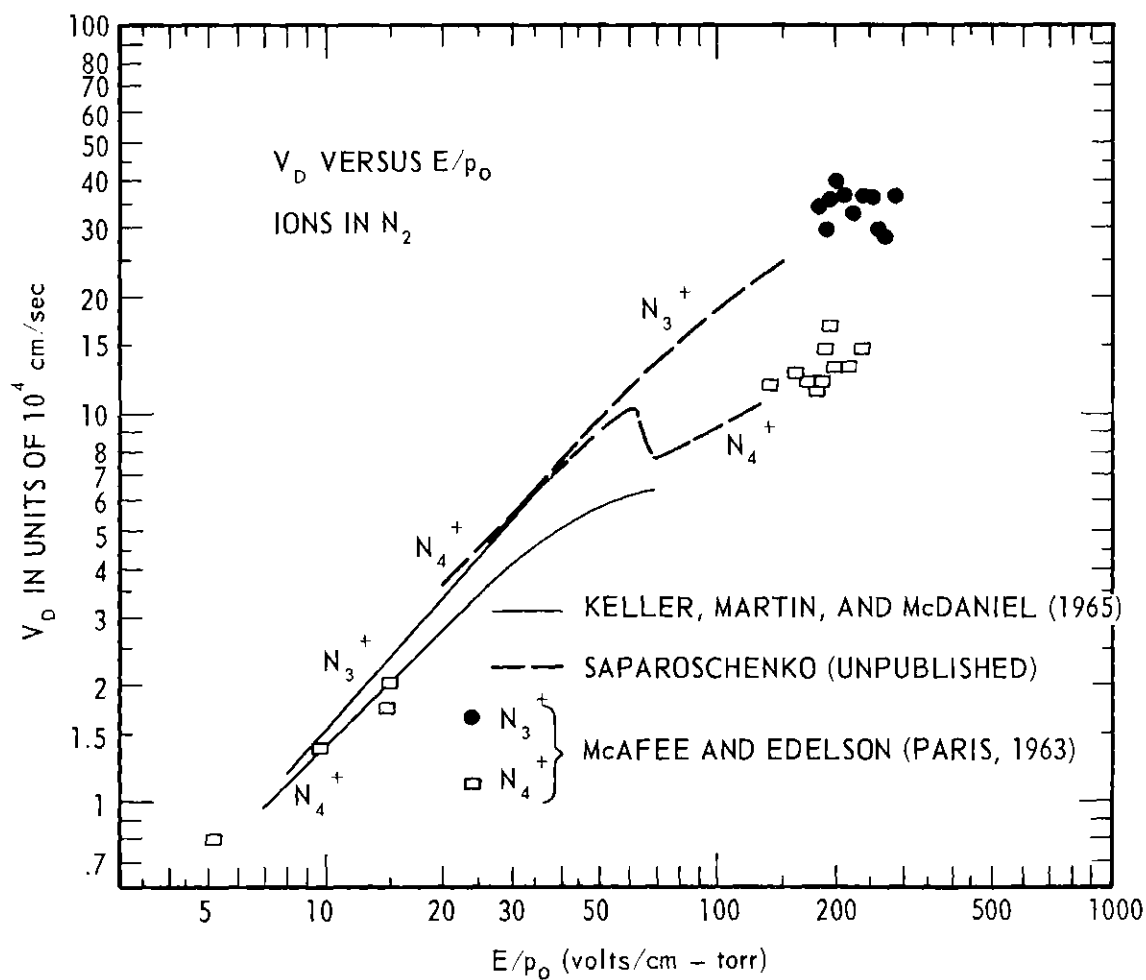


Figure 11. Comparison of Mass-Analyzed Drift Velocity Data - N_3^+ and N_4^+ .

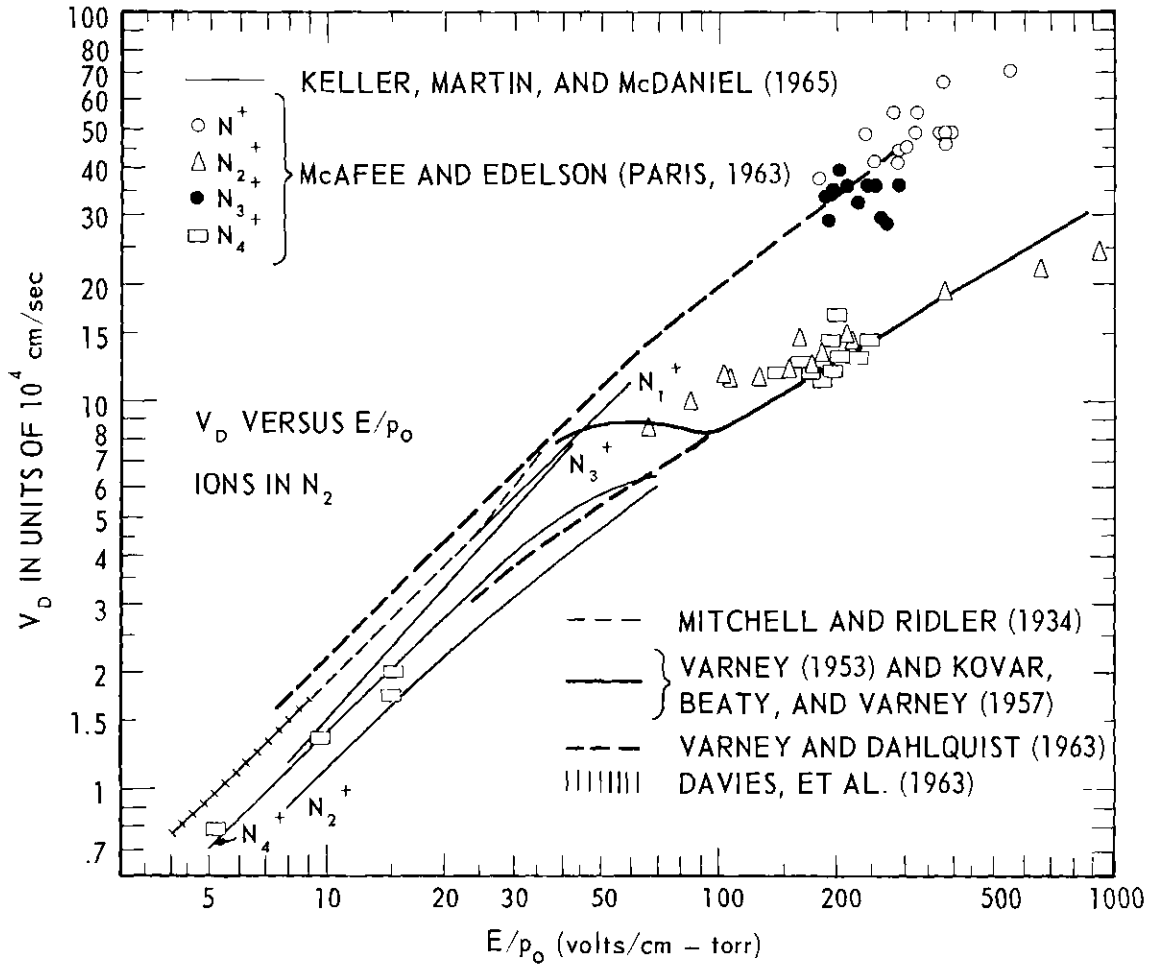


Figure 12. Comparison of Present Data with Data of Other Workers.

zero-field, reduced mobility for N_1^+ of 2.47 can be inferred from the data with some confidence.

In the cases of N_2^+ and N_4^+ , the drift velocity data are scattered from a line of unit slope for certain combinations of pressure and E/p_0 . The arrival time spectra for these two ions exhibit considerable width and overlap. These facts suggest that for low pressure (less than 100 μ) and low E/p_0 , the reaction forming N_2^+ from N_4^+ (Equation 24) predominates, and that the N_4^+ ions that were seen under these conditions were N_2^+ ions for a considerable part of their drift. The low pressure, low E/p_0 data for N_2^+ are consistent with a zero-field, reduced mobility of 1.44. The data of Figures 7-9 suggest that for high pressure (above 150 μ) and low E/p_0 , the reaction forming N_4^+ from N_2^+ (Equation 24) predominates, and that the N_2^+ ions that were seen under these conditions were N_4^+ ions for a considerable part of their drift. The high pressure, low E/p_0 data for N_4^+ are consistent with a zero-field, reduced mobility of 1.84.

There was no pressure regime nor range of E/p_0 in which the drift velocity data for N_3^+ had a slope of unity, so that no zero-field, reduced mobility is implied for N_3^+ . For the higher pressures used in this experiment (150 μ to 200 μ), the drift velocity data for N_3^+ were linear. The fact that the drift velocity data for N_3^+ rise toward the data for N_1^+ for high E/p_0 and fall toward the data for N_4^+ and N_2^+ for low E/p_0 suggest that the N_3^+ ions may have been involved in reactions with these other ions, but the data of this experiment give no clue to the details of such reactions.

The absolute agreement of these data with those of Saporoschenko⁵⁶ and with those of McAfee and Edelson⁴¹ is quite good, except for N_4^+ . Saporoschenko's data show N_4^+ faster than N_3^+ for extremely low E/p_0 . The results of the present experiment contradict Saporoschenko's observation; the present data (Figures 7-9) indicate that N_4^+ is always slower than N_3^+ . Saporoschenko is the only other experimenter who has measured the drift velocities of mass-identified ions in nitrogen at E/p_0 low enough for close comparison with the present results. His apparatus has a one centimeter drift space connected by a 0.004-in.-diameter exit aperture to a mass spectrometer. He uses gas pressures of 500 μ to 1600 μ .

The preliminary data of this experiment that were presented in Paris in 1963⁴¹ lie considerably above the present data. Following the Paris conference, the experiment was improved in a number of ways. Several changes were made in the hookup of the McLeod gauge, the principal one of which was the installation of a cold trap specifically designed to eliminate the effects of thermal transpiration. A number of minor changes were also made in the instrumentation of the experiment. It is a remarkable fact that each and every one of these changes produced the same effect, that of lowering the data. The relative values of the present data for the ions are in good agreement with those of the Paris data. Since then, the scatter of the data has been sharply decreased, and new details have been discovered.

The absolute agreement of these data with the recent results of Woo³⁶ is poor. A great many qualitative features of Woo's drift velocity data are in agreement with the data of this experiment. However, his lack of a mass spectrometer to help him "unscramble" the complications

in nitrogen, his short drift space with the accompanying very brief drift times, and the difficulty of analyzing the data of a mobility experiment of that type made his over-all data analysis extremely difficult, so that some absolute disagreement between his data and the present data might be expected.

The absolute agreement of these data with the theoretical predictions of the Langevin theory¹⁰ is poor. Disagreement with the Langevin predictions could be explained if the point charge-induced dipole interaction were not the dominant one in the case of nitrogen ions drifting through nitrogen gas. In addition, the theory strictly applies only to the case of monatomic ions drifting in a monatomic gas, which is not the case in nitrogen. The present data for N_2^+ agree quite well with Dalgarno's²² quantum-mechanical mobility calculation, which considered resonance charge exchange.

The agreement of the present data with data of other experimenters who do not mass-analyze their ions is not necessarily expected, since their implied mobilities are probably weighted averages for more than one species of ion.

The Pertinent Ion-Molecule Reactions

The data of this experiment are valuable not only for their absolute values but also for their implications concerning the various ion-molecule reactions in nitrogen and the possible influence of such reactions on previous experiments with nitrogen performed by other workers.

Appearance Potentials. The following summary of recent measurements of appearance potentials for the ions in nitrogen is included to aid in understanding the formation of these ions.

<u>Investigator</u>	<u>Date</u>	<u>N₁⁺</u>	<u>N₂⁺</u>	<u>N₃⁺</u>	<u>N₄⁺</u>	<u>Comment</u>
Saporoschenko ⁵⁷	1958	24.2	15.5	22.1	15.8 eV	
Kaul & Fuchs ⁵⁸	1960	24.4	15.6	21.7		
Curran ⁵⁹	1963		15.56	21.04	15.04	Retarding Potential Difference Method
Comes & Lessmann ⁶⁰	1964	24.3	15.576			Photoionization
Llewellyn & Glick ⁶¹	1964	24.3	15.6			R. P. D. Method

Formation. The most likely mode of formation of N₁⁺ is dissociative ionization of a nitrogen molecule. This reaction is described by the equation



Since the appearance potential for N₁⁺ is greater than for any other ion in nitrogen, it has not been thought to be the principal ion in any other mobility experiment. It has been suggested⁶² that N₁⁺ is a secondary ion, whose formation in ordinary mass spectrometric studies involves ions adsorbed on the walls of the ion source of the mass spectrometer; however, in the present work, the ions which were observed were formed not in a closed box, but rather in open space; no exit aperture of the ion source had to be traversed. The arrival time spectra imply that the N₁⁺ ions that were seen were all formed at the source. Although the ionic intensity drops sharply when the electron

energy is reduced, N_1^+ ions have been observed in the present experiment with the electron accelerating voltage as low as about 27 volts. (For lower electron energies the currents of all ions became so small that no useful data could be obtained, so it was not practical to determine if N_1^+ disappeared selectively for energies less than 24.3 eV.)

The initial formation of N_2^+ in the present experiment takes place by the reaction



In the present experiment, the close relationship between N_2^+ and N_4^+ seems to verify the additional formation mechanism of N_2^+ proposed by Varney:⁴



The data of the present experiment suggest that this reaction takes place strongly for low pressures and high E/p_0 .

The formation of N_3^+ is thought to be most likely to take place by the reaction^{57,63,64}



The cross section for this reaction has been measured by Giese and Maier⁶⁵ to be about $0.2 \times 10^{-16} \text{ cm}^2$. Another reaction that has been suggested^{66,42} is:



The reaction seems less likely to be primarily responsible for N_3^+ because the appearance potential of N_3^+ is now quite well established to be less than that for N_1^+ . The binding energy of N_3^+ against dissociation into N_2^+ and N has been estimated to be 3.8 eV by Briglia⁶⁷ and 3.60 eV by Franklin, et al.⁶⁸ The binding energy of N_3^+ against dissociation into N_2 and N_1^+ has been estimated to be 2.8 eV by Briglia⁶⁷ and 2.56 eV by Franklin, et al.⁶⁸

Three different reactions have been proposed for the formation of N_4^+ . The first of these is the second reaction of the pair proposed by Varney:⁴



where the N_4^+ possesses vibrational excitation. The cross section for this reaction has been estimated by Giese and Maier⁶⁵ to be less than $0.003 \times 10^{-16} \text{ cm}^2$. At pressures above 100 μ or 200 μ , it is expected that N_4^+ comes additionally from the reaction^{63,50}



In the last few years some investigators have leaned toward the reaction^{63,59}



where N_2^* is an electronically excited, neutral nitrogen molecule. The analogy with the principal formation mechanism of N_3^+ may be noted. The

results of the present experiment imply that the first of these reactions plays a part, but the present results can shed no light on the second and third reactions.

Some investigators have failed to find any trace of N_4^+ . It may be that their instruments were not sensitive enough to see these ions, but it is more likely that the low binding energy, 0.5 eV^{32} , of N_4^+ played a part. The low binding energy makes N_4^+ considerably easier to dissociate than N_3^+ .

In the present experiment, the most abundant ion at every pressure and at every value of E/p_0 was N_1^+ . This surprising result can probably be explained by noting that the electron energy used throughout these experiments was 75 eV, about three times the energy at the appearance potential for N_1^+ .

If only N_2^+ , N_3^+ , and N_4^+ are considered, N_2^+ dominated for low pressure and high E/p_0 , while N_3^+ and N_4^+ in about equal numbers took over for high pressures (100 μ to 200 μ) and low E/p_0 . The same picture has been seen by several investigators of afterglows.^{69,70,71}

It was hoped that the results of the present experiment could be used to identify "the" ion whose mobility was measured in past experiments in nitrogen without mass analysis. However, the present results clearly indicate how badly one could mislead oneself in attempting to do so. It is true that almost all previously measured mobilities fall between the extreme values 2.47 and 1.44 found here, but the relative concentrations of the various ions in nitrogen are found to be strongly dependent on the type of ion source, the pressure, and E/p_0 . Only an

experiment which includes simultaneous mass analysis can hope to obtain unambiguous mobilities for the ions of a gas as complicated as nitrogen, if such results are indeed possible.

CHAPTER IV

CONCLUSIONS

a. In the present experiment, four ions of the parent gas are seen in nitrogen: N_1^+ , N_2^+ , N_3^+ , and N_4^+ .

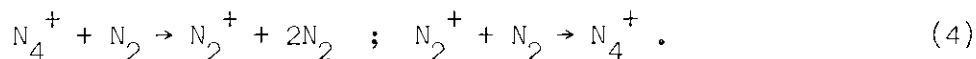
b. For all available conditions N_1^+ is the most abundant ion. This fact is probably the result of the use of electrons of 75-eV energy in the electron bombardment ion source. Most experiments utilize a smaller electron energy, in some cases less than the 24.3 eV necessary⁵⁸ for direct production of N_1^+ ions.

c. The shapes of the arrival time spectra obtained suggest that the N_1^+ ions that are seen are formed only at the source and not farther down the drift tube by secondary processes involving other ions.

d. Over wide limits of pressure and for E/p_0 between 7 and 70 volts/cm-torr the log-log plot of v_d vs E/p_0 for N_1^+ is straight and has a slope of unity. The shape and position of this plot imply a zero-field, reduced mobility for N_1^+ of $2.47 \text{ cm}^2/\text{V-sec}$.

e. Of the other ions (N_2^+ , N_3^+ , and N_4^+), N_2^+ is the most abundant for high E/p_0 , especially for pressures less than about 100μ . N_3^+ and N_4^+ , in about equal numbers, take over from N_2^+ for low E/p_0 provided that the pressure is greater than about 145μ .

f. The shapes of the arrival time spectra show that N_2^+ and N_4^+ are closely interrelated. The widths and overlap of these peaks suggest a reaction scheme of the type proposed by Varney in 1953:



g. The shapes of the arrival time spectra suggest that there may be some reactions between N_3^+ and N_2^+ , and between N_3^+ and N_4^+ .

h. Provided that the gas pressure is less than about 100 μ , the log-log plot of v_d vs E/p_o for N_2^+ is straight and has a slope of unity for E/p_o less than 30 volts/cm-torr. This plot is consistent with a zero-field, reduced mobility for N_2^+ of 1.44 $\text{cm}^2/\text{V-sec}$. For pressures greater than about 145 μ , the plot of v_d vs E/p_o for N_2^+ rises with greatly increased scatter toward the plot of v_d for N_4^+ for E/p_o less than 30 volts/cm-torr.

i. Provided that the gas pressure is greater than about 145 μ , the log-log plot of v_d vs E/p_o for N_4^+ is straight and has a slope of unity for E/p_o less than 30 volts/cm-torr. This plot is consistent with a zero-field, reduced mobility for N_4^+ of 1.84 $\text{cm}^2/\text{V-sec}$. For pressures less than about 100 μ , the plot of v_d vs E/p_o for N_4^+ falls with increased scatter toward the plot of v_d for N_2^+ for E/p_o less than 30 volts/cm-torr.

j. In no available pressure regime is the slope of the log-log plot of v_d vs E/p_o for N_3^+ equal to unity, so that no unique reduced mobility is implied, though for the highest pressures used (150 μ to 200 μ) the drift velocity plot is straight. For pressures less than 100 μ , the plot of v_d for N_3^+ falls toward the plot for N_4^+ .

CHAPTER V

RECOMMENDATIONS

New Drift Tube

The drift velocity measurements made with the present drift tube are almost certainly both accurate and suggestive of the presence of reactions that had been postulated. However, the impurities which persisted all through the experiments prevented further exploration of the results of time arrival spectra or intensity comparisons. Therefore, it is recommended that a new, clean drift tube be built, employing modern vacuum technology to achieve background pressures of the order of 10^{-9} torr. Bakability of a new drift tube should reduce the remaining impurities to a negligible level.

Better Pressure Measurement and Control

The growing awareness of the difficulties produced by cold-trapping a McLeod gauge suggests that modifications need to be made in this area. It is recommended that one of the new, commercially available, capacitance manometers be installed between the drift tube and the McLeod gauge. Thus pressures could be read to the accuracy of the McLeod gauge without cold traps. The output of the capacitance manometer could be used as the input to a vacuum controller, and thus the drift tube pressure could be maintained at any predetermined value for a period of many hours or even days.

New Time Analyzer

Even with the modifications that have been made, the present time analyzer is not always reliable. Its circuits use vacuum tubes; its engineering is not such as to prevent these tubes from going bad at a brisk rate. Further, it has only 20 channels and no built-in time delay. It is recommended that a new, solid-state time analyzer be purchased from among several excellent ones on the market today. It should have about 100 channels and a time-delay feature so that the channels could be used to maximum efficiency. This added resolution might permit meaningful calculations of the diffusion coefficient and mobility simultaneously.

APPENDIX A

ERRORS IN PRESSURE MEASUREMENTS INTRODUCED BY
COLD TRAPPING A MERCURY MANOMETER

There are two main sources of error introduced by adding a cold trap between a system whose pressure is to be measured and a mercury manometer, e. g. a McLeod gauge.⁷² The first source is the Gaede mercury-pumping effect; the second source is the effect of thermal transpiration.

Mercury Pumping

The Gaede mercury-pumping effect⁵¹ has been extensively investigated in the last few years.^{52,53,54} The effect arises from the streaming of mercury vapor from the mercury reservoir of the gauge to the cold trap. The heavy mercury molecules collide with the molecules of the gas whose pressure is being measured (the "sample" gas), and the collisions cause some of the sample gas to be "pumped" from the region of the mercury reservoir toward the region of the cold trap. Thus the mercury stream functions just like an inverted mercury diffusion pump. The result of the pumping action is that the pressure of the sample gas in the region of the mercury reservoir, which is the gas pressure that the gauge measures, is lower than the gas pressure in the region of the cold trap and main vacuum system. The percentage by which the pressure measured is low has been calculated for a few gases.⁵³ These calculations show that if the pressure to be read is less than 10^{-3} torr, where the

mercury vapor pressure is a significant fraction of the total pressure, the error may be of the order of tens of per cent; if the pressure to be read is above 50 μ , the error is less than two per cent.

Thermal Transpiration

The error caused by the effect of thermal transpiration has not been so extensively investigated, probably because the error can be entirely eliminated by use of a suitably designed cold trap⁴⁸.

To understand the effect of thermal transpiration, consider two volumes, V_1 and V_2 , containing a gas at absolute temperatures T_1 and T_2 respectively, which are separated by a partition which is a perfect heat insulator and which has a hole in it. If the diameter of the hole is much greater than the scattering mean free path of the gas, so that the gas flow regime is viscous (see Appendix C), the pressure in the two volumes is the same, i.e.

$$p_1 = p_2, \quad (1)$$

If, however, the diameter of the hole is small compared to the scattering mean free path of the gas (so that a molecule which passes from one side to the other has a negligible chance of returning before it has undergone many collisions and thus attained temperature equilibrium) a different pressure equilibrium is obtained. In this case the number of molecules passing through a hole of area A per second from V_1 to V_2 is $1/4 A n_1 \bar{v}_1$,⁷³ where n_1 is the number density in volume V_1 and \bar{v}_1 is the mean velocity of particles in V_1 . The number of molecules per second

passing from V_2 to V_1 is $1/4 An_2\bar{v}_2$. At equilibrium,

$$n_1\bar{v}_1 = n_2\bar{v}_2 ,$$

$$\frac{n_1\bar{v}_1^2}{\bar{v}_1} = \frac{n_2\bar{v}_2^2}{\bar{v}_2} ,$$

and since $p_i \sim n_i kT_i \sim n_i\bar{v}_i^2$,

$$\frac{p_1}{\bar{v}_1} = \frac{p_2}{\bar{v}_2} ,$$

and thus the pressure equilibrium for this case is expressed by the equation

$$\frac{p_1}{p_2} = \sqrt{\frac{T_1}{T_2}} . \quad (2)$$

This analysis is much more difficult if the two volumes are connected by a tube whose diameter is much less than the scattering mean free path, for the zero-thickness hole in the above analysis is replaced by a tube of finite conductance which has a real temperature gradient along it, but the result is similar to the result expressed by Equation (2).

Consider next a cold trap installed between the main vacuum system, whose gas pressure is to be measured, and the pressure measuring device, e.g. a McLeod gauge. If the gas pressure is such that the scattering mean free path of the gas is comparable to the diameter of the cold trap tubing, the relevant pressure equilibrium is a sensitive

function of the size of the cold trap tubing. In particular, if the cold trap tubing leading to the gauge and the cold trap tubing leading to the system are of different sizes as they leave the cold volume of the trap, the pressure in the system will not necessarily be equal to the pressure in the gauge. The most obvious solution is the use of an ordinary symmetric U-tube cold trap, which eliminates the problem.

When a tube-in-tube trap is used (Figure 13), it is difficult to know what size to make the tubing. Rusch and Bunge⁴⁸ show empirically that the error can be eliminated for tube-in-tube traps if $U_2 A_1 = U_1 A_2$, where U_2 is the total perimeter of the cross section of the annular duct between the two tubes [for a trap of the dimensions shown in Figure 13, $U_2 = \pi(a + b)$], A_2 is the area of the cross section of the annular duct between the two tubes [$A_2 = \pi(a^2 - b^2)$], U_1 is the inside circumference of the small tube, and A_1 is the inside cross-sectional area of the small tube. For a trap of the dimensions shown in Figure 13, this condition becomes $a = b + c$.

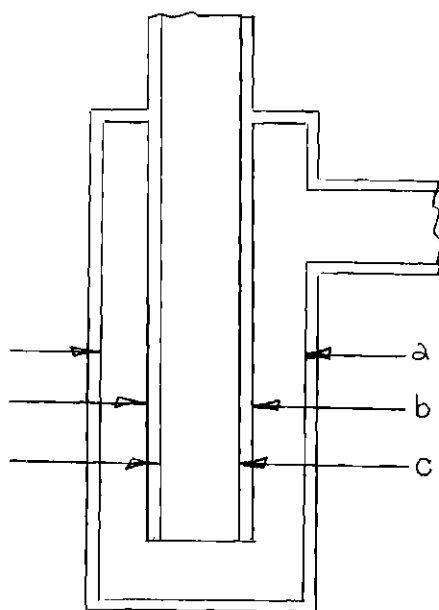


Figure 13
Tube-in-Tube Cold Trap

APPENDIX B

MATHEMATICAL FORM AND EVALUATION OF THE DATA

The information for this appendix is taken from the thesis of William S. Barnes, designated as reference 43. In order to solve the ionic transport problem, it is assumed that the initial spatial shape of the burst of ions created by the ion source could be described by a Dirac delta function. Since this initial condition is physically unrealizable, one should not attempt to extract exact quantitative results from the data for one run. However, it is true that for data with a broad, nearly Gaussian shape the first approximation to the mobility is independent of the diffusion coefficient and reaction rate for that ion. This fact permits one to calculate from the data for each run a mean drift time, and to obtain accurate drift velocities by using differences of these times.

Basic Transport Equation of the System

In formulating and solving the basic equation for the behavior of the ion bursts, the following assumptions are made implicitly or explicitly:

(1) The gas in the drift tube is mainly one kind, with only minute traces of impurities (The level of impurities is not great enough to affect the actual mobility of a given ion appreciably, but reactions with the impurities might affect the mobility measurements by shifting and distorting peaks in the time spectrum),

(2) The gas in the tube has approximately the dielectric coefficient of empty space,

(3) The effects of diffusion may be adequately described by the use of a scalar diffusion coefficient. A diffusion tensor is not necessary,

(4) All magnetic fields are small enough to be ignored,

(5) The geometry of the system is approximately cylindrical, with the z-axis coinciding with the axis of the drift tube,

(6) The ions whose mobilities are being measured are formed in the vicinity of the ion source, that is, either they are primary ions or they are *secondaries* which have been formed near the source in reactions having very large cross sections,

(7) Mutual repulsion plays no significant role,

(8) Ions of the species under consideration may be changed to ions of different species in ion-molecule reactions with neutral molecules of various kinds in the drift tube, but none are created in ion-molecule reactions,

(9) The temperature and pressure of the gas filling the drift tube are constant in space and time.

If the electric field and pressure are such that E/p is low, then the equation of motion of the ion population is given by

$$\underline{J} = -D\nabla n + KEn, \quad (1)$$

where n is the number density of the primary ions under consideration, \underline{J} is the current density of that ion, D is its diffusion coefficient, and K is its mobility. The first term in equation (1) describes the

current density due to diffusion (Fick's law) while the second term gives the expression for the current density due to the migration of ions under the influence of an electric field at low E/p . Strictly speaking this and all subsequent formulas to be derived from it are valid only at low values of E/p . A population of primary ions is also subject to an equation of continuity of the form

$$\nabla \cdot \underline{J} + \sum_i a_i \sigma_i n + \frac{\partial n}{\partial t} = 0, \quad (2)$$

where $\sum a_i \sigma_i n$ represents the combined effect of all ion-molecule reactions using up ions of the species under consideration. The a_i are the rate constants for these reactions, and the σ_i are the number densities of the molecular species with which the ions are reacting. Let $A = \sum a_i \sigma_i$. The combination of equations (1) and (2) gives the partial differential equation describing the transport behavior of the system,

$$-D \nabla \cdot \nabla n + K \nabla \cdot (\underline{E} n) + An + \frac{\partial n}{\partial t} = 0. \quad (3)$$

Solution of the Transport Equation of the System

In view of the assumption of no mutual repulsion, \underline{E} shall be taken as uniform and parallel to the axis of the drift tube. If cylindrical symmetry is assumed then equation (3) becomes, when expressed in cylindrical coordinates,

$$-D \frac{\partial^2 n}{\partial r^2} - \frac{D}{r} \frac{\partial n}{\partial r} - D \frac{\partial^2 n}{\partial z^2} + KE \frac{\partial n}{\partial z} + An + \frac{\partial n}{\partial t} = 0. \quad (4)$$

To separate variables we let

$$n(r,z,t) = R(r) Z(z,t) . \quad (5)$$

Further decomposition of $Z(z,t)$ is not attempted since the particular initial condition that will be applied will produce a solution which is not completely factorable into functions of z and t . The substitution (5) leads to the equation

$$\frac{D}{R} \frac{\partial^2 R}{\partial r^2} + \frac{D}{rR} \frac{\partial R}{\partial r} = - \frac{D}{Z} \frac{\partial^2 Z}{\partial z^2} + \frac{KE}{Z} \frac{\partial Z}{\partial z} + A + \frac{1}{Z} \frac{\partial Z}{\partial t} = -m^2 , \quad (6)$$

where m^2 is a separation constant. One thus obtains the r-equation

$$r^2 \frac{d^2 R}{dr^2} + r \frac{dR}{dr} + s^2 r^2 R = 0 , \quad (7)$$

where

$$s = mD^{-1/2} , \quad (8)$$

and the z-equation

$$-D \frac{\partial^2 Z}{\partial z^2} + KE \frac{\partial Z}{\partial z} + \frac{\partial Z}{\partial t} + (A + s^2 D) Z = 0. \quad (9)$$

The r-equation above [Equation (7)] is the zeroth order Bessel's equation, whose solution is

$$R(r) = C J_0(sr) + F Y_0(sr). \quad (10)$$

For the present work F is set equal to zero, since $Y_0(sr)$ is infinite for r equal to zero.

To solve the z-equation we define a function $f(k,t)$ such that its Fourier transform is $Z(z,t)$:

$$Z(z,t) = \frac{1}{\sqrt{2\pi}} \int_{-\infty}^{\infty} f(k,t) \exp(ikz) dk . \quad (11)$$

Substitution of this expression in the z-equation [Equation (9)] gives a partial differential equation

$$\frac{\partial f(k,t)}{\partial t} + M f(k,t) = 0 , \quad (12)$$

where $M = Dk^2 + ikKE + A + s^2D$. The solution of this equation is

$$f(k,t) = f_0(k) \exp(-Mt) . \quad (13)$$

In this expression $f_0(k)$ is the Fourier transform of the function $Z(z,0)$ which gives the distribution of the ions along the axis of the drift tube when $t = 0$. Hence

$$Z(z,t) = \frac{\exp[-(A + s^2D)t]}{\sqrt{2\pi}} \int_{-\infty}^{\infty} f_0(k) \exp[-Dk^2t + ik(z - KEt)] dk . \quad (14)$$

If the time duration of the square voltage pulse applied to the control plate in the ion source is kept small, the shape of the initial burst of ions may be described, to first approximation, by a Dirac delta function in z . If we let $Z(z,0)$ be a Dirac delta function we will have a normal (bell-shaped) ion distribution in z for all values of t greater than zero. We put $Z(z,0) = N_0 S(z)$, and then $f_0(k) = \frac{N_0}{\sqrt{2\pi}}$, where N_0 is the number of ions in the original burst. Under this assumption, $Z(z,t)$ may be expressed in the form

$$Z(z,t) = Z_1(z,t) + iZ_2(z,t), \quad (15)$$

where

$$Z_1(z,t) = \frac{N_0}{2\pi} \exp[-(A + s^2 D)t] \int_{-\infty}^{\infty} \exp(-Dk^2 t) \cos k(z - KEt) dk \quad (16)$$

and

$$Z_2(z,t) = \frac{N_0}{2\pi} \exp[-(A + s^2 D)t] \int_{-\infty}^{\infty} \exp(-Dk^2 t) \sin k(z - KEt) dk. \quad (17)$$

$Z_2(z,t)$ above is zero since $\exp(-Dk^2 t)$ is an even function of k and $\sin k(z-KEt)$ is odd. $Z_1(z,t)$ may be evaluated by reference to a table of integrals.

$$Z(z,t) = \frac{N_0}{\sqrt{4\pi Dt}} \exp\left[-(A + s^2 D)t - \frac{(z - KEt)^2}{4Dt}\right]. \quad (18)$$

Thus the complete description of the ion density function is given by

$$n(r,z,t) = \frac{N_0}{\sqrt{4\pi Dt}} \sum_i C_i J_0(s_i r) \exp\left[-(A + s_i^2 D)t - \frac{(z - KEt)^2}{4Dt}\right]. \quad (19)$$

To evaluate the s_i it will be assumed that $n(r,z,t)$ is zero at some fixed cylindrical boundary corresponding to some appropriate value of r because of the loss of ions against the electrodes and sides of the drift tube. In the expression (19) above, the Bessel function in the first term will have its first zero at this value of r ; the Bessel function in the second term will have its second zero at this value of r ; etc. The C_i are determined by the initial radial distribution of the ion burst. In this experiment the initial distribution of the ion burst

is not precisely known. The reason that the use of a result [Equation (27)] based on a Dirac delta function model is still considered justified is that any ion cloud initially restricted to a bounded volume of space but otherwise arbitrarily distributed will approach a form represented by the first term of (19) asymptotically with increasing time because of the effect of diffusion.

Normalization of the Distribution in Time

The solution (19) above gives the ion number density throughout the drift tube as a function of r, z , and t . From this density function it is desired to construct a time distribution function for ions passing through the exit aperture of the drift tube. This function, $f(z, t)$, gives the probability that an ion generated at the source at $t = 0$ and passing through the exit aperture will be counted by the mass spectrometer detector between the times t and $t + dt$. Here z is the distance from the source to the exit aperture.

The total number of ions from any given ion burst that eventually pass through the pin-hole is proportional to

$$N(z) = \int_0^{\infty} n(0, z, t) dt, \text{ or} \quad (20)$$

$$N(z) = \frac{N_0}{2\pi} \sum_i C_i \int_0^{\infty} \exp[-(A + s_i^2 D)t] \int_{-\infty}^{\infty} \exp[-Dk^2 t + ik(z - KEt)] dk dt. \quad (21)$$

Integration with respect to time gives

$$N(z) = \frac{N_0}{2\pi} \sum_i C_i \int_{-\infty}^{\infty} \frac{\exp(ikz) dk}{Dk^2 + ikKE + (A + s_i^2 D)}. \quad (22)$$

After D is factored from the denominator of each term in the above series, the denominator may then be written

$$k^2 + ik \frac{KE}{D} + \frac{A + s_i^2 D}{D} = (k - k_1)(k - k_2) ,$$

where

$$k_1 = -\frac{iKE}{2D} \left[1 + \sqrt{1 + 4D \frac{A + s_i^2 D}{K_E^2}} \right] \quad (23a)$$

and

$$k_2 = -\frac{iKE}{2D} \left[1 - \sqrt{1 + 4D \frac{A + s_i^2 D}{K_E^2}} \right] . \quad (23b)$$

Thus the integrand of the above integral has poles on the imaginary axis, one in the upper half-plane and one in the lower. The regime $z > 0$ corresponds to the case where the drift field E is towards the exit aperture. For $z > 0$ a path of integration (Figure 14) may be chosen starting on the real axis at B , going up the real axis to A , and then passing in a semi-circle in the upper half-plane to B . This path passes around the pole at k_2 and the contribution to the integral by the semi-circular part of the path approaches zero as $A \rightarrow +\infty$, $B \rightarrow -\infty$, and as the radius of this path approaches infinity. The residue at k_2 is

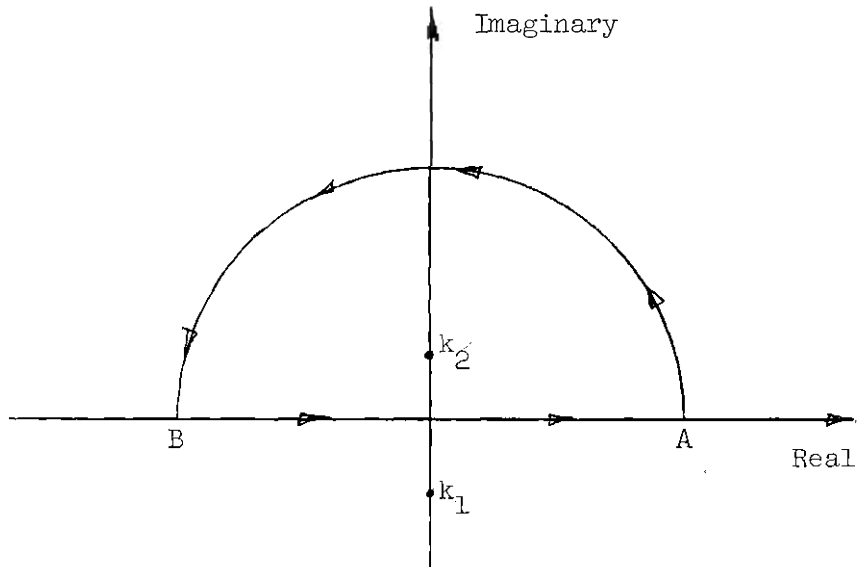


Figure 14. Contour of Integration.

$$R_{12} = -\frac{iD}{KE} \exp \left\{ \left(- \frac{1}{1 + 4D \frac{A + s_i^2 D}{K_E^2}} \right) \left[\frac{zKE}{20} \right] \right\} \quad (24)$$

If we may make the assumption that $K_E^2 \gg 4(A + s_i^2 D)D$ for all s_i 's of importance, then

$$R_{12} = \frac{iD}{KE} \exp \left[- \frac{(A + s_i^2 D)z}{KE} \right] \quad (25)$$

The total number of ions arriving at the exit aperture from any given pulse is proportional to

$$N(z) = \frac{N_0}{KE} \sum_i C_i \exp\left[-\frac{(A + s_i^2 D)z}{KE}\right]. \quad (26)$$

The fraction arriving between t and $t + dt$ is $\frac{n(0,z,t)}{N(z)} dt = f(z,t) dt$.

For any reasonable initial distribution of ions about the source we should have $C_i \ll C_1$ for $i > 1$. Furthermore s_2^2 is approximately four times as large as s_1^2 and the rest of the s_i^2 are even larger so that the higher terms decay and vanish much faster than the first. For a first approximation let us take $C_1 = 1$, $C_i = 0$, for all $i > 1$. This step is equivalent to representing the initial radial distribution by the Bessel function having its first zero at the cylindrical boundary of the system. The result is

$$f(z,t) = \frac{KE}{\sqrt{4\pi Dt}} \exp\left[\frac{(A + s_1^2 D)(z - KEt)}{KE} - \frac{(z - KEt)^2}{4Dt}\right]. \quad (27)$$

Statistical Estimators for K, D, and A

The function (27) above has been put in the form of a statistical distribution having a form which we hope from a priori considerations will represent the distribution of ions according to time of drift. A method frequently used to estimate the parameters of such a distribution function from the experimental distribution of data is called the method of maximum likelihood.⁷⁴

To find the maximum likelihood estimators for K, D, and A we maximize the function

$$L = \log \prod_{i=1}^N f(z, t_i) = \sum_{i=1}^N \log f(z, t_i) \quad (28)$$

by varying parameters. Equating to zero the partial derivatives of L with respect to K , D , and A , we obtain three equations

$$\frac{\partial L}{\partial K} = \frac{N}{K} - \frac{NAz}{K^2 E} - \frac{Ns^2 Dz}{K^2 E} + \frac{NzE}{2D} - \frac{KE^2}{2D} \sum_{i=1}^N t_i = 0, \quad (29)$$

$$\frac{\partial L}{\partial D} = \frac{N}{2D} + \frac{Ns^2 z}{KE} - s^2 \sum_{i=1}^N t_i + \frac{z^2}{4D^2} \sum_{i=1}^N \left[\frac{1}{t_i} \right] - \frac{2NzKE}{4D^2} + \frac{K^2 E^2}{4D^2} \sum_{i=1}^N t_i = 0, \quad (30)$$

$$\frac{\partial L}{\partial A} = \frac{Nz}{KE} - \sum_{i=1}^N t_i = 0. \quad (31)$$

In these equations we substitute

$$\sum_{j=1}^{20} N_j t_j \text{ for } \sum_{i=1}^N t_i \text{ and } \sum_{j=1}^{20} \left[\frac{N}{t_j} \right] \text{ for } \sum_{i=1}^N \left[\frac{1}{t_i} \right].$$

Here N_j is the count recorded in the j th channel and t_j is the time period from the center of the source pulse to the center of the channel interval. In the original formulation (28) each ion counted was assigned its own arrival time, t_i ; the substitution above is made since our data are segregated into 20 classes by the time analyzer according to time of drift. From equation (31) we get

$$K = \frac{z}{E} \frac{N}{20} = \frac{z}{E t} \sum_{j=1}^{20} N_j t_j \quad (32)$$

From the combination of all three equations (29), (30), and (31) we get

$$D = \frac{z^2}{2} \left(\frac{1}{N} \sum_{j=1}^{20} \frac{N_j}{t_j} - \frac{1}{20 \sum_{j=1}^{20} N_j t_j} \right) = \frac{z^2}{2} \left\{ \frac{1}{\bar{t}} - \frac{1}{\bar{t}} \right\} \quad (33)$$

and

$$A = \frac{KE}{z} - s^2 D = \frac{1 + s^2 z^2}{2} \frac{1}{\bar{t}} - \frac{s^2 z^2}{2} \frac{1}{\bar{t}} \quad (34)$$

APPENDIX C

ASPECTS OF RARIFIED GAS DYNAMICS RELEVANT TO THE PRESENT INVESTIGATION

The flow characteristics of a gas in a container are determined by the Knudsen number Kn , which is defined by the equation

$$Kn = \frac{\lambda_s}{d}$$

where λ_s is the scattering mean free path of the molecules of the gas and d is the relevant dimension of the container. When Kn is much greater than unity, the motion of the gas molecules is limited by collisions of the molecules with the container walls, and the gas flow regime is called "free molecular," or simply "molecular." When Kn is much less than unity, the motion of the gas molecules is limited by molecule-molecule collisions, and the gas flow regime is called "continuum," or "viscous." When Kn is about equal to unity, the gas flow regime is called "sliptransition," or simply "transition."⁷⁵ The physics of gas flow in the molecular and the continuum regions is well understood; macroscopic details about the flow in these regions can be obtained from the existing wealth of empirical information in essentially all cases and can even be calculated from basic theoretical considerations in some cases. The flow problem in the transition region is quite a bit more difficult and cannot be treated analytically in most instances.

In an attempt to understand the gas flow dynamics in this experiment, Kn is calculated for each region in the drift tube mass spectrometer:

1. In the drift tube, the pressure is of the order 100μ and the relevant dimensions are of the order of one centimeter so that

$$Kn = \frac{\lambda_s (100\mu)}{1 \text{ cm}} \approx \frac{.08 \text{ cm}}{1 \text{ cm}} = 0.08$$

and the flow is continuum.

2. At the exit aperture of the drift tube,

$$Kn = \frac{\lambda_s (100\mu)}{1/32 \text{ in.}} \approx \frac{.08 \text{ cm}}{.08 \text{ cm}} = 1$$

and the flow is already transitional.

3. In the first differentially pumped chamber, between the exit aperture and the skimmer, the pressure is less than 100μ but most certainly more than 3×10^{-4} torr (see Chapter II). If one assumes that the pressure half-way between the exit aperture and the skimmer aperture is 10^{-3} torr, then Kn at that point is given by the equation

$$Kn = \frac{\lambda_s (10^{-3} \text{ torr})}{1 \text{ to } 2 \text{ cm}} \approx \frac{8 \text{ cm}}{1 \text{ to } 2 \text{ cm}} \approx 6$$

so that the flow is already molecular, and then remains molecular for the remainder of the flight path of the ions.

In the above calculations, it has been assumed that the collisions of interest were of the molecule-molecule and molecule-wall varieties. In this experiment, however, the collisions of interest were those of the ions with gas molecules, for which the mean free path is about four

times shorter than in the molecule-molecule case. Thus, the "ionic Knudsen number" of interest was about four times smaller than the numbers calculated above.

Ideally, ions should suffer no more ion-molecule collisions after they flow through the exit aperture, in order that the ionic population which enters the mass spectrometer be truly representative of the ionic population in the drift tube near the exit aperture. To achieve this condition would have required an infinite pumping speed at the first differentially pumped chamber.

In the present experiment the pumping speed at the first differentially pumped chamber was only 33 liters/sec (see Chapter II), so that there were some ion-molecule collisions in the first chamber. For much of the present work this chamber was as nearly as possible field-free to minimize energetic collisions, i.e. collisions involving ions having more than thermal energy. For a great many of the drift velocity measurements a one-volt positive potential was applied to the exit plate to focus the ions somewhat as they approach the skimmer. This small potential increased the signal intensity at the detector and greatly improved the statistics of the drift velocity data but gave no indication of otherwise affecting the data. Any small end effect on the timing of the ionic flight should not affect the absolute value of the drift velocity data since only differences of mean drift times were used. A more likely effect of the potential applied to the exit aperture plate would be to cause the character of the ions to change in ion-molecule reactions as they traversed the chamber. However, the distance from the drift tube exit aperture to the skimmer aperture is only one or two

centimeters. Also, the energy that an ion has acquired from the field associated with this small potential is smallest near the exit aperture where the pressure is highest and thus the ion-molecule collision rate is highest, and the ion's energy is largest where the collision rate is smallest. Thus the effect of the potential was expected to be small, and that was observed to be the case.

BIBLIOGRAPHY*

1. E. W. McDaniel, Collision Phenomena in Ionized Gases (John Wiley and Son, Inc., New York, 1964), Chap. 9.
2. L. B. Loeb, Basic Processes of Gaseous Electronics (University of California Press, Berkeley, 1960), 2nd ed., Chap. 1.
3. A. M. Tyndall, The Mobility of Positive Ions in Gases (Cambridge University Press, Cambridge, 1938), Chap. 2.
4. R. N. Varney, Phys. Rev. 89, 708 (1953).
5. L. B. Loeb, Basic Processes of Gaseous Electronics (University of California Press, Berkeley, 1960), 2nd ed., Chap. 1, p. 193.
6. E. W. McDaniel, Collision Phenomena in Ionized Gases (John Wiley and Sons, Inc., New York, 1964), Chap. 9, p. 490.
7. P. Langevin, Ann. Chim. Phys. 28, 289 (1903).
8. L. B. Loeb, Basic Processes of Gaseous Electronics (University of California Press, Berkeley, 1960), 2nd ed., Chap. 1, p. 42.
9. E. W. McDaniel, Collision Phenomena in Ionized Gases (John Wiley and Sons, Inc., New York, 1964), Chap. 9, p. 431.
10. P. Langevin, Ann. Chim. Phys. 5, 245 (1905).
11. H. R. Hassé, Phil. Mag. 1, 139 (1926).
12. S. Chapman, Phil. Trans. of Roy. Soc. A216, 279 (1916), A217, 115 (1917). S. Chapman and T. G. Cowling, The Mathematical Theory of Non-uniform Gases (Cambridge University Press, London, 1952), 2nd ed.
13. D. Enskog, Dissertation, Uppsala, 1917.
14. T. Kihara, Rev. Mod. Phys. 24, 45 (1952), 25, 844 (1953).
15. E. A. Mason and H. W. Schamp, Jr., Ann. Phys. (New York) 4, 233 (1958).

* Abbreviations used herein are found in the American Institute of Physics Style Manual (1963).

16. G. H. Wannier, Bell System Tech. J. 32, 170 (1953), #2071. Phys. Rev. 83, 281 (1951), 87, 795 (1952).
17. L. Sena, J. Physics (U.S.S.R.) 10, 179 (1946).
18. J. A. Hornbeck and G. H. Wannier, Phys. Rev. 82, 458 (1951).
19. J. A. Hornbeck, Phys. Rev. 84, 615 (1951).
20. R. N. Varney, Phys. Rev. 88, 362 (1952).
21. A. Dalgarno, M. R. C. McDowell, and A. Williams, Phil. Trans. Roy. Soc. A250, 411 (1958).
22. A. Dalgarno, Phil. Trans. Roy. Soc. A250, 426 (1958).
23. A. M. Arthurs and A. Dalgarno, Proc. Roy. Soc. (London) A256, 540, 552 (1960).
24. A. Dalgarno and R. J. W. Henry, Atomic Collision Processes (edited by M. R. C. McDowell) (North-Holland Publishing Co., Amsterdam, 1964), pp. 914 - 920. This book is the proceedings of the Third International Conference on the Physics of Electronic and Atomic Collisions, London, 1963.
25. A. M. Tyndall and C. F. Powell, Proc. Roy. Soc. A129, 162 (1930).
26. E. C. Beaty, Proceedings of the Fifth International Conference on Ionization Phenomena in Gases, Munich, 1961 (North-Holland, Amsterdam, 1962), Vol. I, p. 183.
27. N. E. Bradbury, Phys. Rev. 40, 508 (1932).
28. J. H. Mitchell and K. E. W. Ridler, Proc. Roy. Soc. (London) A146, 911 (1934).
29. J. H. Hornbeck, Phys. Rev. 83, 374 (1951).
30. F. R. Kovar, E. C. Beaty, and R. N. Varney, Phys. Rev. 107, 1490 (1957).
31. E. C. Beaty, Phys. Rev. 104, 17 (1956).
32. R. N. Varney, J. Chem. Phys. 31, 1314 (1959).
33. R. N. Varney and J. A. Dahlquist, Proceedings of the Sixth International Conference on Ionization Phenomena in Gases, Paris, 1963 (S.F.R.M.A., Paris, 1963), Vol. I, p. 309.

34. R. N. Varney, Atomic Collision Processes (edited by M. R. C. McDowell) (North-Holland Publishing Co., Amsterdam, 1964), p. 877. This book is the proceedings of the Third International Conference on the Physics of Electronic and Atomic Collisions, London, 1963.
35. J. A. Dahlquist, J. Chem. Phys. 39, 1203 (1963).
36. S. B. Woo, Thesis, Washington University, St. Louis, Mo. (1963), unpublished. The bulk of this work has been submitted to J. Chem. Phys. for publication.
37. J. K. Vogel, Z. Physik 148, 355 (1957).
38. P. G. Davis, J. Dutton, and F. Llewellyn-Jones, Atomic Collision Processes (edited by M. R. C. McDowell) (North-Holland Publishing Co., Amsterdam, 1964), p. 877. This book is the proceedings of the Third International Conference on the Physics of Electronic and Atomic Collisions, London, 1963.
39. E. C. Zipf, Jr., private communication.
40. D. W. Martin, W. S. Barnes, G. E. Keller, D. S. Harmer, and E. W. McDaniel, Proceedings of the Sixth International Conference on Ionization Phenomena in Gases, Paris, 1963 (S.E.R.M.A., Paris, 1963), Vol. I, p. 295.
41. K. B. McAfee and D. Edelson, Proceedings of the Sixth International Conference on Ionization Phenomena in Gases, Paris, 1963 (S.E.R.M.A., Paris, 1963), Vol. I, p. 299.
42. D. Wobschall, J. R. Graham, and D. P. Malone, Phys. Rev. 131, 1565 (1963).
43. W. S. Barnes, Thesis, Georgia Institute of Technology (1963), unpublished.
44. E. W. McDaniel, D. W. Martin, and W. S. Barnes, Rev. Sci. Instr. 33, 2 (1962).
45. R. M. Bozarth and others, Permanent Magnet Handbook (Crucible Steel Co. of America, Pittsburg, 1957).
46. E. B. Winn and A. O. Nier, Rev. Sci. Instr. 20, 773 (1949).
47. H. Konig and G. Helwig, Z. Physik 129, 491 (1951).
48. Von M. Rusch and O. Bunge, Z. Tech. Phys. 13, 77 (1932).
49. A. O. Nier, Rev. Sci. Instr. 18, 398 (1947).
50. P. F. Knewstubb and A. W. Tickner, J. Chem. Phys. 37, 2941 (1962).

51. Von W. Gaede, Ann. Physik 46, 357 (1915).
52. H. Ishii and K. Nakayama, Transactions of the Eighth Vacuum Symposium, 1961 (Pergamon Press, Oxford, 1962), Vol. I, p. 519.
53. C. Meinke and G. Reich, Vacuum 13, 579 (1963).
54. E. W. Rothe, J. Vac. Sci. and Tech. I, 66 (1964).
55. E. W. McDaniel, Collision Phenomena in Ionized Gases (John Wiley and Sons, Inc., New York, 1964), Chap. 9, p. 428.
56. M. Saporoschenko, private communication.
57. M. Saporoschenko, Phys. Rev. 111, 1550 (1958).
58. Von W. Kaul and R. Fuchs, Z. Naturforsch., 15A, 326 (1960).
59. R. K. Curran, J. Chem. Phys. 38, 2974 (1963).
60. Von F. J. Comes and W. Lessman, Z. Naturforsch., 19A, 65 (1964).
61. J. A. Llewellyn and R. E. Glick, Florida State University, Bulletin #14, Division of Biology and Medicine, U. S. Atomic Energy Commission, May 1, 1964.
62. C. J. Cook and J. R. Peterson, Phys. Rev. Letters 9, 164 (1962).
63. M. S. B. Munson, F. H. Field, and J. L. Franklin, J. Chem. Phys. 37, 1790 (1962).
64. V. Cermak and Z. Herman, Col. Czech. Chem. Commun. 27, 1493 (1962).
65. C. F. Giese and W. B. Maier II, J. Chem. Phys. 35, 1913 (1961).
66. Von H. Dreeskamp. Z. Naturforsch. 12A, 876 (1957).
67. D. D. Briglia, Phys. Dept. of U.C.L.A., Task No. 860504, 763506, Scientific Report #1, AFCRL-64-259.
68. J. L. Franklin, V. H. Dibeler, R. M. Reese, and M. Drauss, J. Am. Chem. Soc. 80, 298 (1958).
69. W. H. Kasner, W. A. Rogers, and M. A. Biondi, Phys. Rev. Letters 7, 321 (1961).
70. W. L. Fite, J. A. Rutherford, and V. A. J. van Lint, Discussions Faraday Soc. 33, 264 (1962).
71. M. A. Biondi, Annales de Geophysique 20, 34 (1964).

72. P. H. Carr, Vacuum 14, 37 (1964).
73. E. W. McDaniel, Collision Phenomena in Ionized Gases (John Wiley and Sons, Inc., New York, 1964), Chap. 2, p. 44.
74. A. M. Mood, Introduction to the Theory of Statistics (McGraw-Hill Book Company).
75. J. E. Scott, Jr. and J. E. Drewry, Rarified Gas Dynamics (edited by J. A. Laurmann) (Academic Press, Inc., New York, 1963), Vol. 1, p. 516. This book is the proceedings of the Third International Symposium on Rarified Gas Dynamics, Paris, 1963.

VITA

George Emerson Keller was born in Columbia, South Carolina on July 11, 1938. He is the son of Mr. and Mrs. Francis W. Keller. On September 2, 1961, he was married to Alice Everette Rawlinson, also from Columbia.

Mr. Keller was educated in the public schools of Columbia, and graduated from Dreher High School there in 1956. He has received two degrees from the Georgia Institute of Technology, the degree of Bachelor of Science in Physics in June, 1960, and in June, 1962, the degree of Master of Science in Physics. Since January, 1960, he has been a graduate research assistant in the Engineering Experiment Station of the Georgia Institute of Technology.

Mr. Keller is a member of the American Physical Society and of Sigma Xi.